



1 Environmental factors influencing cold-
2 water coral ecosystems in the oxygen
3 minimum zones on the Angolan and
4 Namibian margins
5

6 Ulrike Hanz¹, Claudia Wienberg², Dierk Hebbeln², Gerard Duineveld¹, Marc Lavaleye¹, Katriina
7 Juva³, Wolf-Christian Dullo³, André Freiwald⁴, Leonardo Tamborrino², Gert-Jan Reichart^{1,5},
8 Sascha Flögel³, Furu Mienis¹

9 ¹*NIOZ-Royal Netherlands Institute for Sea Research and Utrecht University, Department of Ocean Systems, Texel,*
10 *1797SH, Netherlands*

11 ²*MARUM—Center for Marine Environmental Sciences, University of Bremen, Bremen, 28359, Germany*

12 ³*GEOMAR Helmholtz Centre for Ocean Research, Kiel, 24148, Germany*

13 ⁴*Department for Marine Research, Senckenberg Institute, Wilhelmshaven, 26382, Germany*

14 ⁵*Faculty of Geosciences, Earth Sciences Department, Utrecht University, Utrecht, 3512JE, Netherlands*

15 *Correspondence to: Ulrike Hanz (ulrike.hanz@nioz.nl), +31222369466*

16

17

18

19

20

21

22



23 Abstract

24 Fossil cold-water coral mounds overgrown by sponges and bryozoans were observed in anoxic
25 conditions on the Namibian margin, while mounds colonized by thriving cold-water coral reefs were
26 found in hypoxic conditions on the Angolan margin. These low oxygen conditions do not meet known
27 environmental ranges favoring cold-water corals and hence are expected to provide unsuitable habitats
28 for cold-water coral growth and therefore reef formation. To explain why the living fauna can
29 nevertheless thrive in both areas, present day environmental conditions at the southwestern African
30 margin were assessed. Downslope CTD transects and the deployment of bottom landers were used to
31 investigate spatial and temporal variations of environmental properties. Temporal measurements in the
32 mound areas recorded oscillating low dissolved oxygen concentrations of 0-0.17 ml l⁻¹ (\pm 0-9 %
33 saturation) on the Namibian and 0.5-1.5 ml l⁻¹ (\pm 7-18 % saturation) on the Angolan margin, which were
34 associated with relatively high temperatures (11.8-13.2°C and 6.4-12.6°C respectively). Semi-diurnal
35 barotropic tides were found to interact with the margin topography producing internal waves with
36 excursions of up to 70 and 130 m for the Namibian and Angolan margins, respectively. These tidal
37 movements temporarily deliver water with more suitable characteristics to the coral mounds from
38 below and above the hypoxic zone. Concurrently, the delivery of high quantity and quality of suspended
39 particulate organic matter was observed, which serves as a food source for cold-water corals. On the
40 Namibian slope organic matter indicates a completely marine source and originates directly from the
41 surface productive zone, whereas on the Angolan margin the geochemical signature of organic material
42 suggest an additional mechanisms of food supply. A nepheloid layer observed above the cold-water
43 coral mound area on the Angolan margin may constitutes a reservoir of fresh organic matter, facilitating
44 a constant supply of food particles by tidal mixing. This suggests that the cold-water coral communities
45 as well as the associated fauna may compensate unfavorable conditions induced by low oxygen levels
46 and high temperatures with an enhanced availability of food. With the expected expansion of oxygen
47 minimum zones in the future due to anthropogenic activities, this study provides an example on how
48 ecosystems could cope with such extreme environmental conditions.

49

50



51 1. Introduction

52 Cold-water corals (CWCs) form 3D structures in the deep-sea, providing important habitats for dense
53 aggregations of sessile and mobile organisms ranging from mega- to macrofauna (Henry and Roberts,
54 2007;van Soest et al., 2007) and fish (Costello et al., 2005). Consequently, CWC areas are considered as
55 deep-sea hotspots of biomass and biodiversity (Buhl-Mortensen et al., 2010;Henry and Roberts, 2017).
56 Moreover, they form hotspots for carbon cycling by transferring carbon from the water column towards
57 associated benthic organisms (Oevelen et al., 2009;White et al., 2012). Some framework-forming
58 scleractinian species, with *Lophelia pertusa* and *Madrepora oculata* being the most common species in
59 the Atlantic Ocean (Freiwald et al., 2004;White et al., 2005;Roberts et al., 2006;Cairns, 2007), are
60 capable of forming large elevated seabed structures, so called coral mounds (Wilson, 1979;Wienberg
61 and Titschack, 2017;Titschack et al., 2015;De Haas et al., 2009). These coral mounds, consisting of coral
62 debris and hemipelagic sediments, commonly reach heights between 20 and 100 m and can be several
63 kilometers in diameter. They are widely distributed along the Atlantic margins, being mainly restricted
64 to water depths between 200-1000 m, while records of single colonies of *L. pertusa* are reported from a
65 broader depth range of 50-4000 m depth (Roberts et al., 2006;Hebbeln et al., 2014;Davies et al.,
66 2008;Mortensen et al., 2001;Freiwald et al., 2004;Freiwald, 2002;Grasmueck et al., 2006;Wheeler et al.,
67 2007).

68 A global ecological-niche factor analysis by Davies et al. (2008) and Davies and Guinotte (2011),
69 predicting suitable habitats for *L. pertusa*, showed that this species generally thrives in areas which are
70 nutrient-rich, well oxygenated and affected by relatively strong bottom water currents. Other factors
71 potentially important for proliferation of *L. pertusa* include chemical and physical properties of the
72 ambient water masses (aragonite saturation state, salinity, temperature) and water depth (Davies et al.,
73 2008;Dullo et al., 2008;Flögel et al., 2014;Davies and Guinotte, 2011). *L. pertusa* is most commonly
74 found at temperatures between 4-12°C and a very wide salinity range between 32 and 38.8 (Freiwald et
75 al., 2004). Although they occur in such a wide range of temperature and salinity, the link of *L. pertusa* to
76 particular salinity and temperature within the NE Atlantic led Dullo et al. (2008) to suggest that they are
77 restricted to a specific density envelope of sigma-theta (σ_θ) = 27.35-27.65 kg m⁻³. In addition, the
78 majority of occurrences of live *L. pertusa* come from sites with dissolved oxygen concentrations (DO_{conc})
79 between 6-6.5 ml l⁻¹ (Davies et al., 2008), with lowest recorded oxygen values being 2.1-3.2 ml l⁻¹ at CWC
80 sites in the Gulf of Mexico (Davies et al., 2010;Schroeder, 2002;Brooke and Ross, 2014) or even as low as
81 1-1.5 ml l⁻¹ off Mauritania where CWC mounds are in a dormant stage showing only scarce living coral
82 occurrences today (Wienberg et al., 2018;Ramos et al., 2017). Dissolved oxygen levels hence seem to



83 affect the formation of CWC structures as also shown by Holocene records obtained from the
84 Mediterranean Sea, which revealed periods of reef demise and growth in conjunction with hypoxia (with
85 2 ml l^{-1} seemingly forming a threshold value for active coral growth; Fink et al., 2012).

86 Another essential constraint for CWC growth and therefore mound development in a generally food
87 deprived deep-sea is food supply. *L. pertusa* is an opportunistic feeder, exploiting a wide variety of
88 different food sources, including phytodetritus, phytoplankton, mesozooplankton, bacteria and dissolved
89 organic matter (Kiriakoulakis et al., 2005; Dodds et al., 2009; Gori et al., 2014; Mueller et al.,
90 2014; Duineveld et al., 2007). Transport of surface organic matter towards CWC sites at intermediate
91 depths has been found to involve either active swimming (zooplankton), passive sinking, advection, local
92 downwelling, and internal waves and associated mixing processes resulting from interactions with
93 topography (Davies et al., 2009; van Haren et al., 2014; Thiem et al., 2006; White et al., 2005; Mienis et al.,
94 2009; Frederiksen et al., 1992). Not only quantity but also quality of food particles is of crucial
95 importance for the uptake efficiency as well as ecosystem functioning of CWCs (Ruhl, 2008; Mueller et
96 al., 2014).

97 With worldwide efforts to map CWC communities, *L. pertusa* has also been found under conditions
98 which seem environmentally stressful or extreme in the sense of the global limits defined by Davies et
99 al. (2008) and Davies and Guinotte (2011). Examples are the warm and salty waters of the
100 Mediterranean and the high temperature variations along the US coast (Cape Lookout; Freiwald et al.,
101 2009; Mienis et al., 2014; Taviani et al., 2005). Environmental stress generally increases energy needs for
102 organisms to recover and maintain optimal functioning, which accordingly increases their food demand
103 (Sokolova et al., 2012). For the SW African margin one of the few records of living CWC come from the
104 Angolan margin (at 7° ; Le Guilloux et al., 2009), which raises the question whether local environmental
105 factors limit CWC growth due to the presence of an Oxygen Minimum Zone (OMZ; see Karstensen et al.
106 2008), or data is lacking. Hydroacoustic campaigns nevertheless revealed extended areas off Angola and
107 Namibia with structures that morphologically resemble coral mounds structures known from the NE
108 Atlantic (M76-3, MSM20-1; Geissler et al., 2013; Zabel et al., 2012).

109 Two such mound areas on the margins off Namibia and Angola were visited during the RV *Meteor* cruise
110 M122 'ANNA' (ANGola/NAMibia) cruise in January 2016 (Hebbeln et al., 2017). During this cruise fossil
111 CWC mound structures were observed near Namibia, while flourishing CWC reef covered mound
112 structures were observed on the Angolan margin. The aim of the present study was to assess present-
113 day environmental conditions at the southwestern African margin that enable cold-water coral growth



114 in this low oxygen environment. To identify key parameters influencing CWC growth and therefore
115 mound development, hydrographic parameters as well as chemical properties of the water column were
116 measured, characterizing environmental conditions and food supply. These data are used to provide
117 new insights in susceptibility of CWCs towards extreme oxygen limited environments, in order to
118 improve understanding of the fate of CWC mounds in a changing ocean.

119 2. Material and Methods

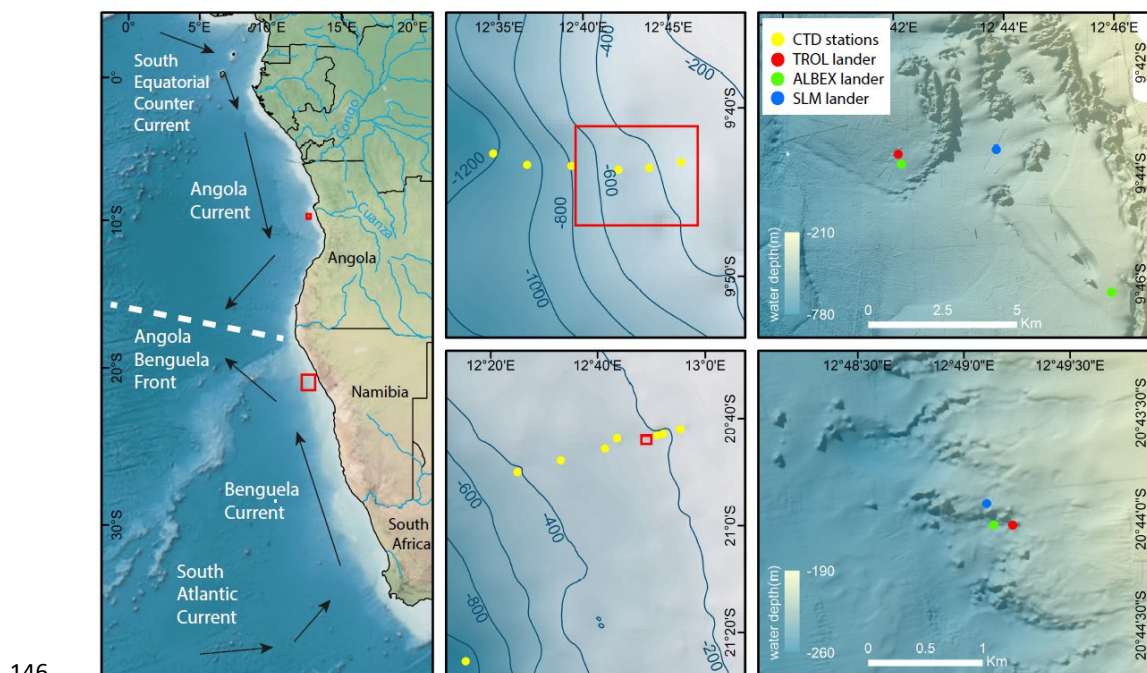
120 2.1 Setting

121 2.1.1 Oceanographic setting

122 The SW African margin is one of the four major eastern boundary regions in the world and is
123 characterized by upwelling of nutrient-rich cold waters (Shannon and Nelson, 1996). The availability of
124 nutrients triggers a high primary production, making it one of the most productive marine areas
125 worldwide with an estimated production of 0.37 Gt C/yr (Carr and Kearns, 2003). Remineralization of
126 high fluxes of organic particles settling through the water column result in severe mid-depth oxygen
127 depletion and an intense OMZ over large areas along the SW African margin (Chapman and Shannon,
128 1985). The extension of the OMZs is highly dynamic being controlled by upwelling intensity which
129 depends on the prevailing winds and two current systems along the SW African margin, i.e. the Benguela
130 and the Angola currents (Kostianoy and Lutjeharms, 1999; Chapman and Shannon, 1987; Fig. 1). The
131 Benguela Current originates from the South Atlantic Current, which mixes with water from the Indian
132 Ocean at the southern tip of Africa (Poole and Tomczak, 1999; Mohrholz et al., 2008; Rae, 2005) and
133 introduces relatively cold and oxygen-rich Eastern South Atlantic Central Water (ESACW; Poole and
134 Tomczak 1999) to the SW African margin (Mohrholz et al., 2014). The Angola Current originates from the
135 South Equatorial Counter Current and introduces warmer, nutrient-poor and less oxygenated South
136 Atlantic Central Water (SACW; Poole and Tomczak 1999) to the continental margin (Fig. 1a). While the
137 SACW flows along the continental margin the oxygen concentration is decreasing continuously due to
138 remineralisation processes on the SW African shelf (Mohrholz et al., 2008). Both currents converge at
139 around 14-16 °S, resulting in the Angola-Benguela Front (Lutjeharms and Stockton, 1987). In austral
140 summer, the Angola-Benguela Front can move southward to 23 °S (Shannon et al., 1986), thus
141 increasing the influence of the SACW along the Namibian coast (Junker et al., 2017; Chapman and
142 Shannon, 1987), contributing to the pronounced OMZ due to its low initial oxygen concentration (Poole
143 and Tomczak, 1999). ESACW is the dominant water mass at the Namibian margin during the main



144 upwelling season in austral winter, expanding from the oceanic zone about 350 km offshore, further in-
145 shore. (Mohrholz et al., 2014).



146
147 **Figure 1** (a) Overview map showing the research areas off Angola and Namibia (red squares) and main features of the surface
148 water circulation (arrows) and frontal zone (dashed line) in the SE Atlantic as well as the two main rivers discharging at the
149 Angolan margin. Detailed bathymetry maps of the Angolan (upper maps) and Namibian margins (lower maps) showing the
150 position of (b) CTD transects (note the deep CTD cast down to 1000 m water depth conducted off Namibia) and (c) bottom
151 lander deployments (red squares shown in (b) indicate the cutouts displayed in (c)).

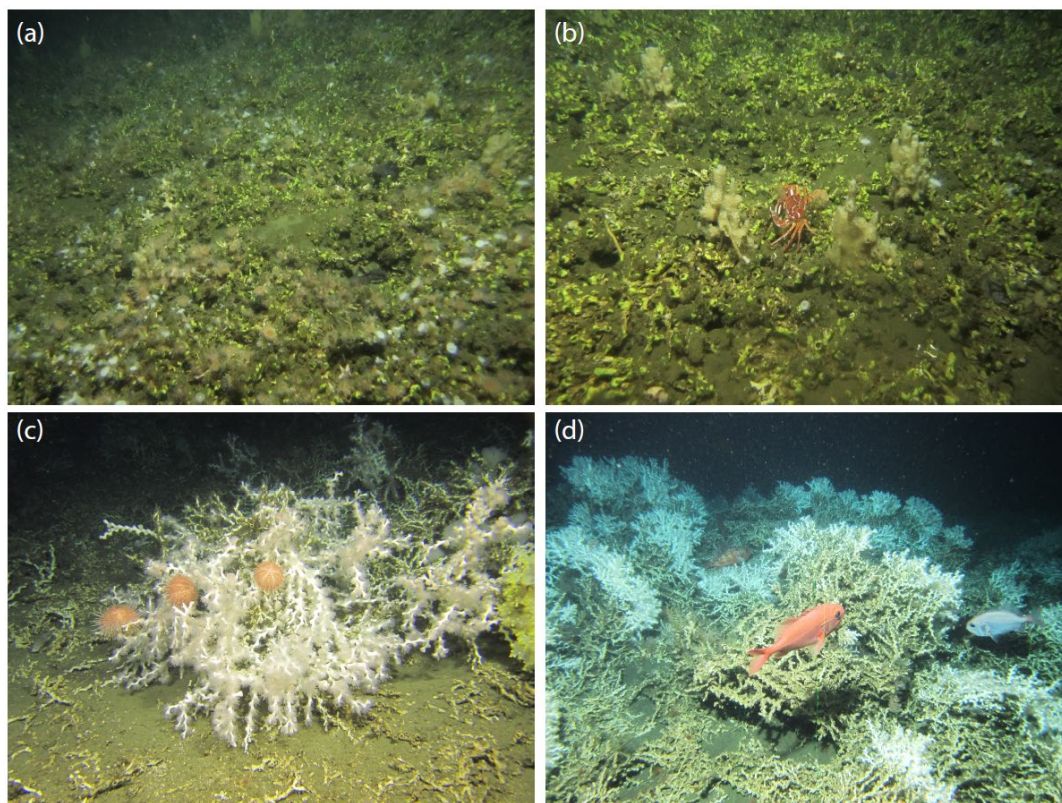
152 2.1.2. Coral mound provinces along the Angolan and Namibian margins

153 During RV *Meteor* cruise M122 in 2016, over 2000 coral mounds were observed between 160-260 m
154 water depth on the Namibian shelf (Hebbeln et al., 2017). All mounds were densely covered with coral
155 rubble and dead coral framework (entirely consisting of *L. pertusa*), while no living corals were observed
156 in the study area (Hebbeln et al., 2017; Figs. 2a, b). Few species were locally very abundant, viz. a yellow
157 cheilostome bryozoan which was the most common species, and five sponge species. The bryozoans
158 were encrusting the coral rubble, whereas some sponge species reached heights of up to 30 cm (Fig. 2a,
159 b). The remaining CWC community consisted of an impoverished fauna overgrowing *L. pertusa* debris.
160 Commonly found sessile organism were actinarians, zoanths, hydroids, some thin encrusting sponges,
161 serpulids and sabellid polychaetes. The mobile fauna comprised asteroids, ophiuroids, two shrimp



162 species, amphipods, cumaceans and holothurians. Locally high abundances of *Suffogobius bibarbatus*, a
163 fish that is known to be adapted to hypoxic conditions, were observed in cavities underneath the coral
164 framework (Hebbeln, 2017). Corals collected from the surface of various Namibian mounds date back to
165 about 5 ka BP, pointing to a simultaneous demise of these mounds during the mid-Holocene
166 (Tamborrino et al., submitted).

167 On the Angolan margin CWC structures varied from individual mounds to long ridges. Some mounds
168 reached heights of more than 100 m above the seafloor. At shallow depths (~250 m) also some isolated
169 smaller mounds are present (Hebbeln et al. 2017). All mounds showed thriving CWC cover, which was
170 dominated by *L. pertusa* (estimated 99% relative abundance), *M. oculata* and solitary corals. Mounds
171 with a flourishing coral cover were mainly situated at water depths between 330-470 m, whereas single
172 colonies were found over an even broader depth range between 250-500 m (Figs. 2c, d; Hebbeln et al.,
173 2017). Additionally to CWCs, large aggregations of hexactinellid sponges (*Aphrocallistes*, *Sympagella*)
174 were observed. The scattered small mounds at shallower water depths were dominated by sponges and
175 only sparsely covered with living coral. In these areas, active suspension feeders, like sponges were most
176 commonly observed. First estimates for coral ages obtained from a gravity core records collected at one
177 of the Angolan coral mounds revealed continuous coral mound formation during the last 34 ka until
178 today (Wefing et al., 2017).



179

180 **Figure 2** ROV images (copyright MARUM ROV SQUID, Bremen, Germany) showing the surface coverage of cold-water coral
181 mounds discovered off Namibia (a, b) and Angola (c, d). Images were recorded and briefly described for their faunal
182 composition during RV *Meteor* cruise M122 "ANNA" (see Hebbeln et al. 2017). (a) Sylvester mound, 225 m water depth. Dead
183 coral framework entirely consisting of *Lophelia pertusa*. The framework is intensely colonized by the yellow bryozoan
184 *Metropriella* sp., zoanithids, actinarians and sponges. Vagile fauna consists of asteroids and gobiid fishes (*Sufflogobius*
185 *bibarbatus*) that hide between hollows underneath the coral framework. (b) Sylvester mound, 238 m water depth. Dense coral
186 rubble (*L. pertusa*) heavily overgrown by *Metropriella* sp. and sponges. Note the decapod crab *Macropipus australis* (center of
187 the image). (c) Valentine mound, 238 m water depth. Live *Lophelia* colony being grazed by echinoids. Note the sponge
188 *Aphrocallistes* sp. with its actinarian symbionts (right side of the image). (d) Buffalo mound, 345 m water depth. Living CWC
189 reef observed on top of an Angolan coral mound. Many fishes are present around the reef (*Helicolenus dactylopterus*,
190 *Gephyroberyx darwinii*).

191 **2.2 Methodology**

192 During RV *Meteor* expedition M122 in January 2016, two CTD transects and five short-term bottom
193 lander deployments (Table 1, Fig. 1) were carried out to measure near-bed environmental conditions



194 potentially influencing benthic habitats. In addition, weather data were continuously recorded by the RV
195 *Meteor* weather station, providing real-time information on local wind speed and wind direction.

196 *2.2.1 Lander deployments*

197 Sites for deployment of the NIOZ designed landers (ALBEX and TROL) were selected based on multibeam
198 bathymetric data. In each area, two landers were deployed simultaneously. On the Namibian margin
199 one lander was deployed on top of a mound structure (water depth 220 m), while the other lander was
200 deployed in close vicinity but off-mound (Fig. 1, Table 1). As both landers show similar trends for all
201 measured physical properties, only the dataset recorded by the ALBEX lander is presented here (see
202 Table 1). Off Angola, mounds with live corals were observed over a large depth zone (250-500 m). To
203 obtain as much information as possible over the entire mound zone, one lander (ALBEX) was first
204 deployed in the relatively shallow part of the mound zone at 340 m water depth, and after retrieval
205 redeployed in the deeper part of the zone at 530 m. A second lander (TROL) was deployed at the
206 deeper part of the zone (530 m) for the full time period (Fig. 1, Table 1). Since the records of the ALBEX
207 and TROL landers obtained during the simultaneous deployment at the deep mound site (~530 m) did
208 not show significant differences, only the data of the ALBEX lander are here presented (Table 1). These
209 data are compared with ALBEX lander data obtained during its deployment in the shallow part of the
210 mound zone at ~340 m (Table 1). Deployment times varied from 2.5 to 8 days (Table 1).

211 Both, the ALBEX and TROL lander consist of an aluminum tripod for this experiment equipped with 13
212 glass benthos floats, two IXSEA acoustic releasers and a single 260 kg ballast weight. Oceanographic data
213 were obtained by different sensors: an ARO-USB oxygen sensor (JFE-Advantech™) which also recorded
214 temperature, a combined OBS-fluorometer (Wetlabs™) and an Aquadopp (Nortek™) profiling current
215 meter. The ALBEX lander was furthermore equipped with a Technicap PPS4/3 sediment trap with 12
216 bottles (allowing daily samples) and a McLane particle pump (24 filter units for each 7.5 L of seawater,
217 two hour interval) to sample particulate organic matter in the near-bottom water (40 cm above
218 bottom).

219 Additionally, a GEOMAR Satellite Lander Module (SLM) was deployed off-mound close to the NIOZ
220 landers (Fig. 1, Table1). The SLM was equipped with a 600 kHz ADCP Workhorse Sentinel 600 from RDI, a
221 CTD (SBE SBE16V2™), a combined fluorescence and turbidity sensor (WET Labs ECO-AFL/FL), a dissolved
222 oxygen sensor (SBE™) and a pH sensor (SBE™) (Hebbeln et al., 2017). From the SLM only pH
223 measurements are used here, complementing the data from the NIOZ landers.

224



225 2.2.2 CTD transects

226 Vertical profiles of principal hydrographic parameters in the watercolumn, viz. temperature,
227 conductivity, oxygen and turbidity, were obtained using a Seabird CTD/Rosette system (Seabird SBE 9
228 plus). The additional sensors on the CTD were a dissolved oxygen sensor (SBE 43 membrane-type DO
229 Sensor) and a combined fluorescence and turbidity sensor (WET Labs ECO-AFL/FL). The CTD was
230 combined with a rosette water sampler consisting of 24 Niskin® water sampling bottles (10 L) that were
231 electronically triggered to close at given depths during the up-cast. CTD casts were carried out along two
232 downslope CTD transects (Fig. 1). Off Angola, the downslope transect covered a distance of 20 km
233 reaching down to a depth of 800 m, whereas the main transect in Namibia covered a distance of 60 km
234 and maximum depth of 400 m. In order to measure deeper water masses, one deep CTD cast was
235 conducted at a distance of about 130 km from the shallowest CTD, going down to about 1000 m depth
236 (Figs. 1 and 3).

237 2.2.3 Hydrographic data processing

238 The CTD dataset was processed using the processing software Seabird data SBE 11plus V 5.2 and data
239 were visualized using the program Ocean Data View (Schlitzer 2011; Version 4.7.8). Turbidity data were
240 only collected on the Angolan slope.

241 Hydrographic data recorded by the CTD and landers were analyzed and plotted using the program R
242 (Team, 2017). Data from the different instruments (temperature, turbidity, current speed, oxygen
243 concentration, fluorescence) were averaged over a period of 1.5 h to remove shorter tem trends and
244 occasional spikes. Correlations between variables were assessed by Spearman's rank correlation tests.

245 2.2.4 Suspended particulate matter

246 With each upcast of the CTD/Rosette, water samples were taken as close to the seabed as possible, at
247 mid-water depth, and in the chlorophyll-maximum. From each depth, two 5 L water samples were
248 subsequently filtered over pre-combusted (450 °C) and pre-weighted GF/F filters (47 mm, Whatman™).
249 Filters were stored at -20 °C until further analysis at the NIOZ.

250 Near-bottom suspended particulate organic matter (SPOM) was additionally sampled by means of a
251 phytoplankton sampler (McLane PPS) mounted on the ALBEX lander. The PPS was fitted with 24 GF/F
252 filters (47 mm Whatman™ GF/F filters pre-combusted at 450 °C). A maximum of 7.5 L was pumped over
253 each filter during a 2h period yielding a time series of near bottom SPOM supply and its variability over a
254 period of 48 hours.



255 *C/N analysis and isotope measurements*

256 Filters from the in situ pump and sampled from the CTD/Rosette were freeze-dried before further
257 analysis. Half of each filter was used for phytopigment analysis and a ¼ section of each filter was used
258 for analyzing organic carbon, nitrogen, and their stable isotope ratios. The filters, used for carbon
259 analysis, were decarbonized by vapor of concentrated hydrochloric acid (2 M HCl supra) prior to
260 analyses. Filters were transferred into pressed tin capsules (12x5 mm, Elemental Microanalysis) and
261 $\delta^{15}\text{N}$, $\delta^{13}\text{C}$ and total weight percent of organic carbon and nitrogen were analyzed by a Delta V
262 Advantage isotope ratio MS coupled on line to an Elemental Analyzer (Flash 2000 EA-IRMS) by a Conflo
263 IV (Thermo Fisher Scientific Inc.). The used reference gas was purified atmospheric N_2 . As a standard for
264 $\delta^{13}\text{C}$ benzoic acid and acetanilide was used, for $\delta^{15}\text{N}$ acetanilide, urea and casein was used. For $\delta^{13}\text{C}$
265 analysis a high signal method was exercised including a 70% dilution. Values are reported relative to v-
266 pdb and the atmosphere respectively. Precision and accuracy based on replicate analyses and
267 comparing international standards for $\delta^{13}\text{C}$ and $\delta^{15}\text{N}$ was ± 0.15 ‰. The C/N ratio is based on the weight
268 ratios between TOC and N.

269 *Phytopigments*

270 Phytopigments were measured by reverse-phase high-performance liquid chromatography (RP-HPLC)
271 with a gradient based on the method published by (Kraay et al., 1992). For each sample half of a GF/F
272 filter was used and freeze-dried before extraction. Pigments were extracted using 95% methanol and
273 sonification. All steps were performed in a dark and cooled environment. Pigments were identified by
274 means of their absorption spectrum, fluorescence and the elution time. Identification and quantification
275 took place as described by Tahey et al. (1994). The absorbance peak areas of chlorophyll- α were
276 converted into concentrations using conversion factors determined with a certified standard. The
277 $\Sigma\text{Phaeopigment/ Chlorophyll-}\alpha$ ratio gives an indication about the degradation status of the organic
278 material, since phaeopigments form as a result of bacterial or autolytic cell lysis and grazing activity
279 (Welschmeyer and Lorenzen, 1985).

280 *2.2.5 Tidal analysis*

281 The barotropic (due to the sea level and pressure change) and baroclinic (internal „free waves“
282 propagating along the pycnoclines) tidal signals obtained by the Aquadopp (Nortek™) profiling current
283 meter were analysed from the bottom pressure and from the horizontal flow components recorded 6 m
284 above the sea floor, using the harmonic analysis toolbox `t_tide` (Pawlowicz et al., 2002). The data mean
285 and trends were subtracted from the data before analysis.

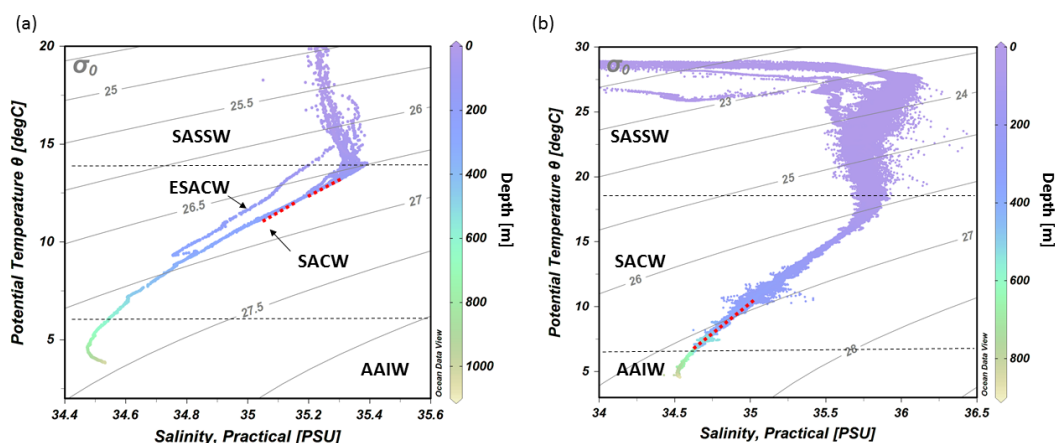


286 3. Results

287 3.1 Namibian margin

288 3.1.1 Water column properties off Namibia

289 The hydrographic data obtained by CTD measurements along a downslope transect from the surface to
290 1000 m water depth revealed distinct changes in temperature and salinity through the water column.
291 These are ascribed to the different water masses in the study area (Fig. 3a). In the upper 85 m of the
292 water column, temperatures are above 14°C and salinities are > 35.2, which corresponds to South
293 Atlantic Subtropical Surface Water (SASSW). SACW is situated underneath the SASSW and reaches down
294 to about 700 m. SCAW is defined by a linear relationship between temperature and salinity in the TS-
295 plot (Shannon et al., 1987). The temperature in the layer of SCAW decreases from 14 to 7°C with depth
296 and the salinity from 35.4 to 34.5 (Fig. 3a). The deep CTD cast about 130 km from the coastline recorded
297 a water mass with the signature of ESACW, having a lower temperature (-1.3°C) and lower salinity (-0.2
298 PSU) than SACW (in 200 m depth, not included in CTD transects of Fig. 4). Underneath these two central
299 water masses Antarctic Intermediate Water (AAIW) was found with a temperature <7°C.



300

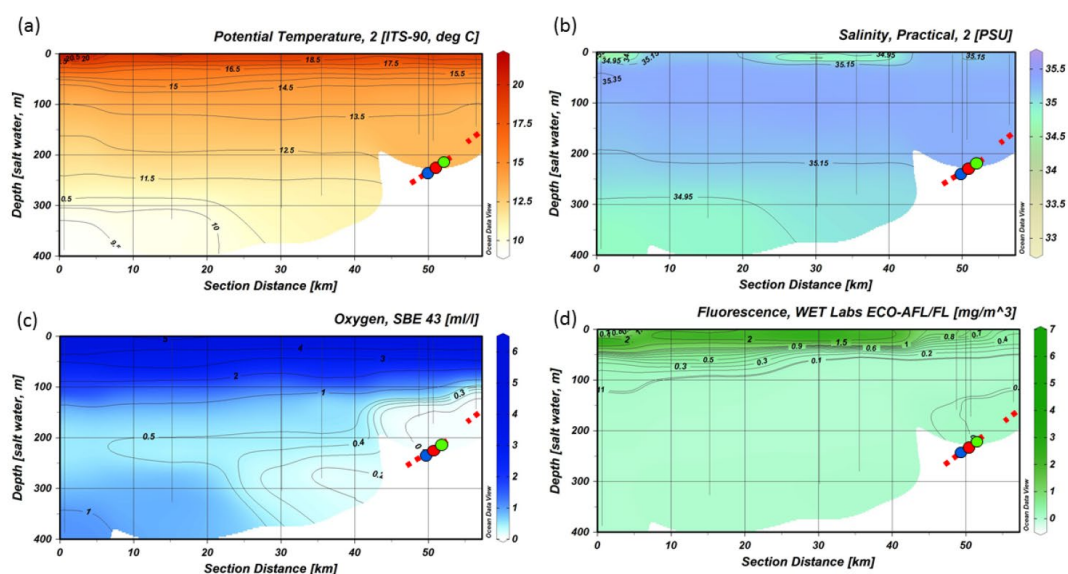
301 **Figure 3** TS-diagrams showing the different water masses being present at the (a) Namibian and (b) Angolan margins: South
302 Atlantic Subtropical Surface Water (SASSW), South Atlantic Central Water (SACW) and Eastern South Atlantic Central water
303 (ESACW), Antarctic Intermediate Water (AAIW) (data plotted using Ocean Data View v.4.7.8; <http://odv.awi.de>; Schlitzer, 2011).
304 Red dotted line indicates the depth range of cold-water coral mound occurrence.

305 The CTD transect showed decreasing DO_{conc} from the surface (6 ml l^{-1}) towards a minimum in 150-200 m
306 depth (0 ml l^{-1}). Lowest values for DO_{conc} were found on the continental margin between 100-335 m
307 water depth. The DO_{conc} in this pronounced OMZ ranged from $<1 \text{ ml l}^{-1}$ down to 0 ml l^{-1} ($\cong 9-0 \%$)



308 saturation, respectively). The zone of low DO_{conc} ($<1 \text{ ml l}^{-1}$) was stretching horizontally over the complete
 309 transect towards at least 100 km offshore (Fig. 4c). The upper boundary of the OMZ was relatively sharp
 310 compared to its lower limits and corresponds with the border between SASSW at the surface and SACW
 311 below.

312 Within the OMZ, a small increase in fluorescence (0.2 mg m^{-3}) was recorded, whereas fluorescence was
 313 otherwise not traceable below the surface layer (Fig. 4d). Within the surface layer highest surface
 314 fluorescence ($>2 \text{ mg m}^{-3}$) was found $\sim 40 \text{ km}$ offshore. Above the center of the OMZ fluorescence
 315 reached only up to 0.4 mg m^{-3} .



316
 317 **Figure 4** CTD transect across the Namibian margin. Shown are data for: (a) potential temperature ($^{\circ}\text{C}$), (b) salinity (PSU), (c)
 318 dissolved oxygen concentrations (ml l^{-1}), note the pronounced oxygen minimum zone (OMZ) between 100-335 m water depth,
 319 and d) fluorescence (mg m^{-3}) (data plotted using Ocean Data View v.4.7.8; <http://odv.awi.de>; Schlitzer, 2011). The occurrence of
 320 fossil CWC mounds is indicated by a red dashed line, colored dots indicate bottom lander deployments.

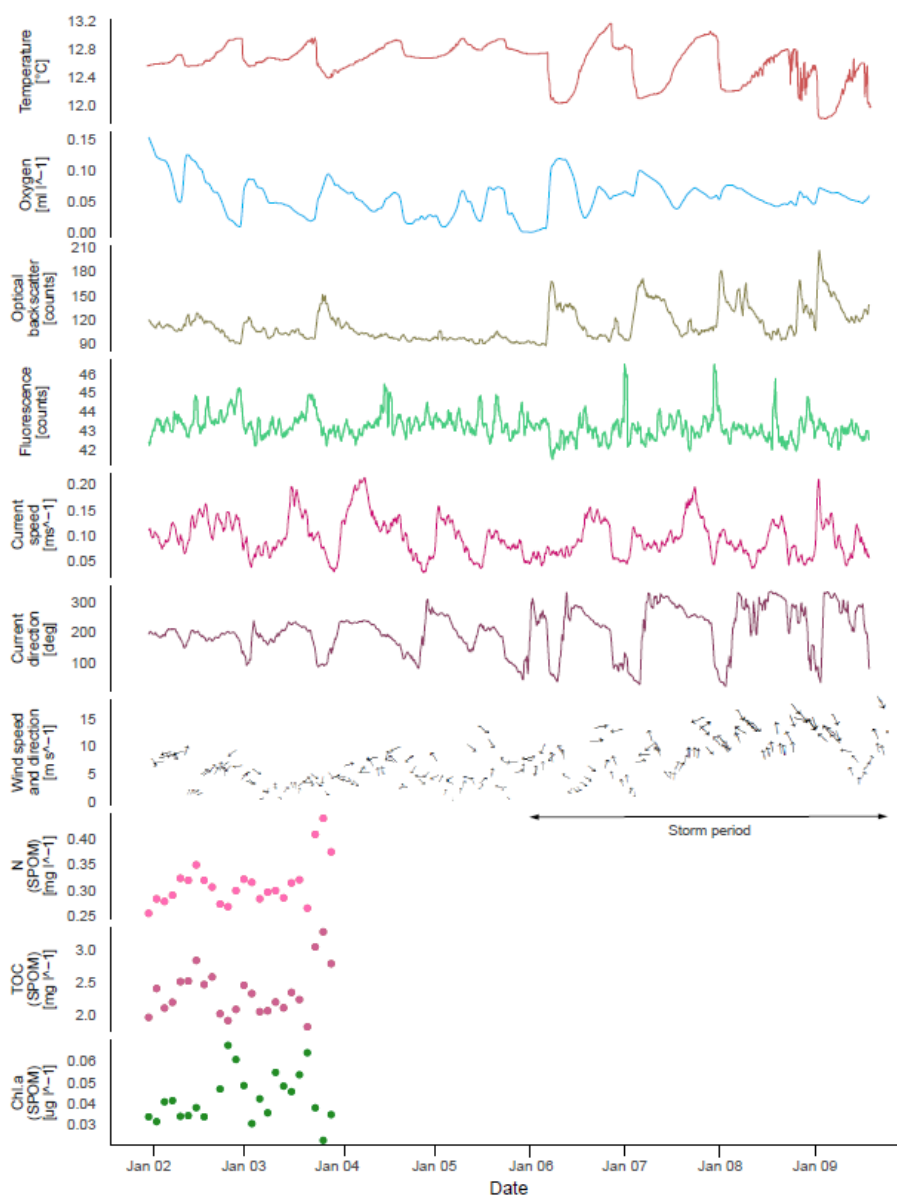
321 3.1.2 Lander time-series of physical data

322 Bottom temperature ranged from 11.8 to 13.2°C during the deployment of the ALBEX lander (Table 1)
 323 showing oscillating fluctuations with a maximum semidiurnal ($\Delta t \sim 6 \text{ h}$) change of $\sim 1^{\circ}\text{C}$ (on 9.1.2018). The
 324 DO_{conc} fluctuated between 0 - 0.15 ml l^{-1} and was negatively correlated with temperature ($r=-0.39$,
 325 $p<0.01$). Fluorescence ranged from 42 to 45 NTU during the deployment and was positively correlated
 326 with temperature ($r=0.38$, $p<0.01$). Hence, both temperature and fluorescence were negatively



327 correlated with oxygen concentration ($r=-0.39$, $p<0.01$) and also with turbidity (optical backscatter, $r=-$
328 0.35 , $p<0.01$). Turbidity was relatively low until it increased especially during the second half of the
329 deployment, when wind speeds increased and also the current direction changed. The maximum current
330 speeds measured during the deployment period were 0.21 m s^{-1} , with average current speeds of 0.09 m
331 s^{-1} (Table 2). The tidal cycle explains $>80\%$ of the pressure fluctuations (Table 2), with a semidiurnal
332 signal, M2, generating an amplitude of >0.35 dbar and thus being the most important constituent.
333 Before the 6th of January the current direction oscillated between SW and SE where after it changed into
334 a dominating northern current direction. The current speed remained rather constant during the
335 deployment period (Fig. 5). The wind speed, on the other hand, increased from 10 m s^{-1} to a maximum
336 of 17 m s^{-1} on the sixth of January and remained high for the next six days. Wind direction changed from
337 anticlockwise cyclonic rotation towards alongshore winds. The water current direction returned to SW-
338 SE after the period of strong wind (not shown). During the strong wind period, colder water (correlation
339 between wind speed and water temperature, $r=-0.55$, $p<0.01$), with a higher turbidity (correlation of
340 wind speed and turbidity, $r=0.42$, $p<0.01$) and higher DO_{conc} was present. The SLM lander recorded an
341 average pH of 8.01.

342 The observed fluctuations in bottom water temperature at the deployment site imply a vertical tidal
343 movement of around 70 m. This was calculated by comparing the temperature change recorded by the
344 lander to the respective temperature-depth gradient based on water column measurements (CTD site
345 GeoB20553, $12.58 \text{ }^\circ\text{C}$ at 245 m, $12.93 \text{ }^\circ\text{C}$ at 179 m). Due to these vertical tidal movements, the oxygen
346 depleted water from the core of the OMZ is regularly being replaced with somewhat colder and slightly
347 more oxygenated water (up to 0.2 ml l^{-1}).



348

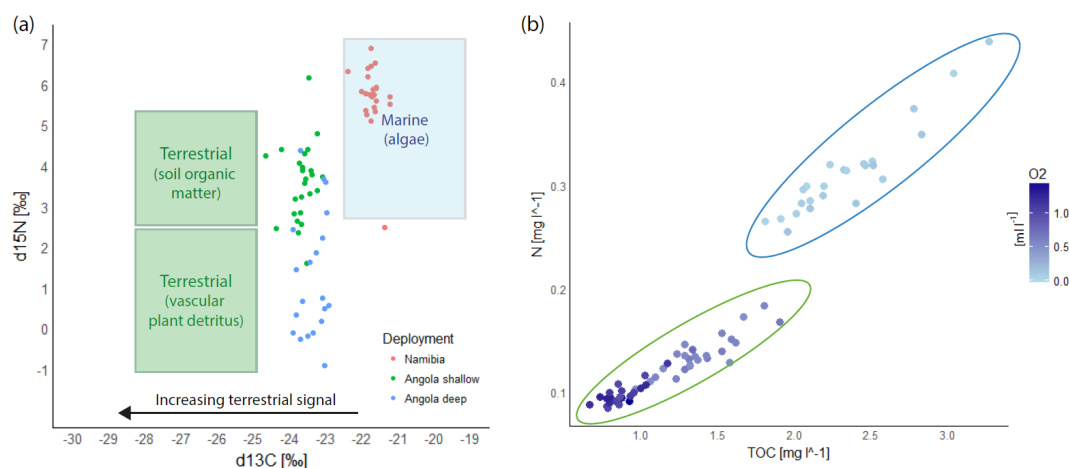
349 **Figure 5** Data recorded by the ALBEX lander (210 m) at the Namibian margin in January 2016. Shown are data for temperature
350 (°C; red), dissolved oxygen concentrations (ml l^{-1} ; blue), optical backscatter (turbidity; moss green), fluorescence (counts per
351 second green), current speed (m s^{-1} ; pink), current direction (degree: 0-360°; dark red) as well as nitrogen (mg l^{-1} ; pink dots),
352 carbon (mg l^{-1} ; purple dots), and chlorophyll- α concentration ($\mu\text{g l}^{-1}$; green dots) of SPOM collected during the first 48h by the
353 McLane pump. These data are supplemented by wind speed and direction (small black arrows) recorded concurrently to the
354 lander deployment by ship bound devices. Note that current directions changed from a generally south-poleward to an
355 equatorward direction when wind speed exceeded 10 m s^{-1} (stormy period indicated by black arrow).



356 3.1.3 Food supply

357 The nitrogen (N) concentration of the SPOM measured on the filters of the ALBEX lander McLane pump
358 fluctuated between 0.25 and 0.45 mg l⁻¹ (Fig 5). The highest N concentration corresponded with a peak
359 in turbidity ($r=0.42$, $p<0.01$). The $\delta^{15}\text{N}$ values of the lander time series fluctuated between 5.1 and 6.9
360 with an average value of 5.7 ‰. Total Organic Carbon (TOC) showed a similar pattern as nitrogen, with
361 relative concentrations ranging between 1.8-3.5 mg l⁻¹. The $\delta^{13}\text{C}$ value of the TOC increased during the
362 surveyed time period from -22.39 to -21.24‰ with an average of -21.7 ‰ (Fig. 6a). The C/N ratio ranged
363 from 8.5 to 6.8 and was on average 7.4 (Fig. 6b). During periods of low temperature and more turbid
364 conditions TOC and N as well as the $\delta^{13}\text{C}$ values of the SPOM were higher.

365 Chlorophyll- α concentrations in the SPOM collected with the lander in situ pump were on average 0.042
366 $\mu\text{g l}^{-1}$ and correlated with the record of the fluorescence sensor on the Seabird CTD ($r=0.43$, $p=0.04$). A
367 six times higher amount of chlorophyll- α degradation products were found during the lander
368 deployment (0.248 $\mu\text{g l}^{-1}$) compared to the amount of chlorophyll- α , giving a $\Sigma\text{Phaeopigment/}$
369 Chlorophyll- α ratio of 6.5 (not shown). Additionally, carotenoids (0.08-0.12 $\mu\text{g l}^{-1}$) and fucoxanthin (0.22
370 $\mu\text{g l}^{-1}$) were found as major components of the pigment fraction, which are common in diatoms.
371 Zeaxanthin, indicating the presence of prokaryotic cyanobacteria, was only observed in small quantities
372 in the SPM (0.066 $\mu\text{g l}^{-1}$).



373

374 **Figure 6** Composite records of SPOM collected by the McLane pump of the ALBEX lander at the Namibian and Angolan margins
375 during all three deployments. (a) $\delta^{15}\text{N}$ and $\delta^{13}\text{C}$ isotopic values at the Namibian (red dots) and Angolan (blue and green dots)
376 margins. Indicated by the square boxes are common isotopic values of terrestrial and marine organic matter (Boutton 1991,
377 Holmes et al. 1997, Sigman et al. 2009). The relative contribution of terrestrial material (green boxes) is increasing with a more



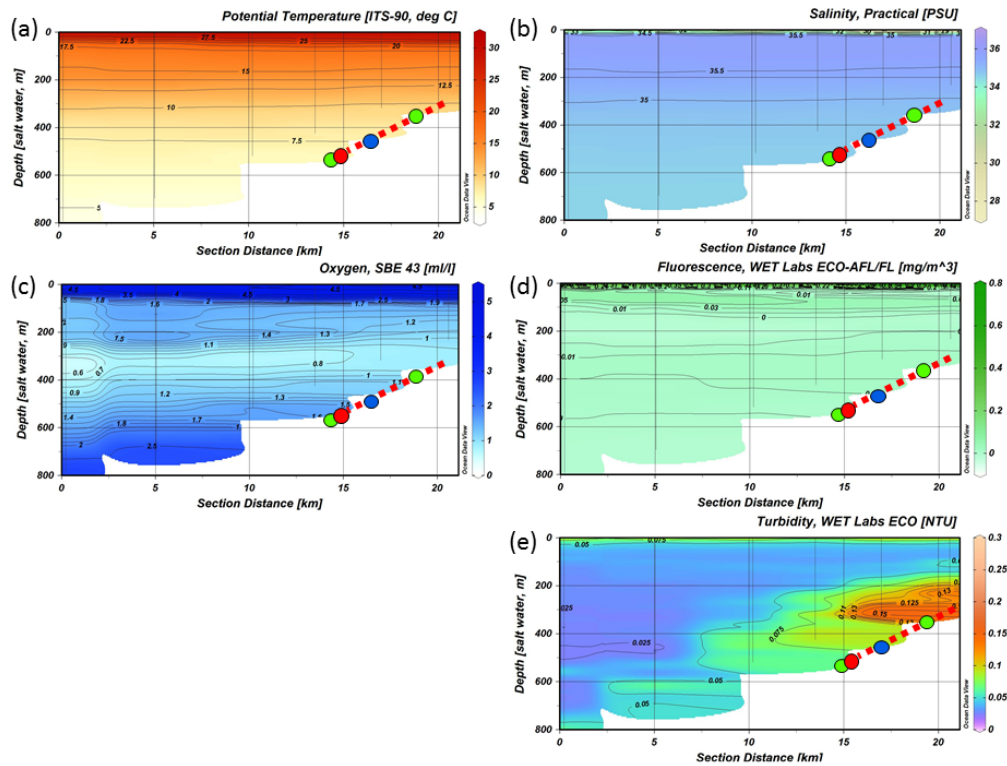
378 negative $\delta^{13}\text{C}$ value. (b) Total organic carbon (TOC) and nitrogen (N) concentration of the SPOM. Values of the Namibian
379 margin are marked by a blue circle (C/N ratio = 7.8), values of the Angolan margin are marked by a green circle (C/N ratio = 9.6).
380 Dissolved oxygen concentrations are included to show the higher nutrient concentrations in less oxygenated water.

381 3.2 Angolan margin

382 3.2.1 Water column properties

383 The hydrographic data obtained by CTD measurements along a downslope transect from the surface to
384 800 m water depth revealed distinct changes in temperature and salinity throughout the water column,
385 related to four different water masses. At the surface a distinct shallow layer (>20 m) with a distinctly
386 lower salinity (27.3-35.5) and higher temperature (29.5-27 °C, Fig. 3b) was observed. Below the surface
387 layer, SASSW was recognized down to a depth of 70 m, characterized by a higher salinity (35.8). SACW
388 was observed between 70-600 m, featuring the expected linear relationship between temperature and
389 salinity. Temperature and salinity decreased from 17.5°C/35.8 to 7°C/34.6. At 700 m depth AAIW was
390 recorded, characterized by a low salinity (<34.4) and temperature (<7°C, Fig. 3b).

391 The CTD transect shows a sharp decrease in the DO_{conc} underneath the SASSW from 5 to <2 ml l^{-1} (Fig. 7).
392 DO_{conc} was further decreasing until a minimum of 0.6 ml l^{-1} at 350 m and subsequently increasing to >3
393 ml l^{-1} at 800 m depth. Lowest DO_{conc} were not found at the slope but 70 km offshore in the center of the
394 zone of reduced DO_{conc} between 200-450 m water depth (<1 ml l^{-1}). Compared to the Namibian margin
395 (see Fig. 4), the hypoxic layer was hence situated further offshore, slightly deeper and overall DO_{conc}
396 were higher (compare Fig. 4c). Also, the boundaries of the hypoxic zone were not as sharp. Salinity
397 underneath the surface layer decreased linearly from 35.75 to 34.5 in 800 m and did not show any
398 specific features likewise as the temperature which decreased from 16 to 5°C. Fluorescence near the sea
399 surface was generally low (around 0.2 with small maxima of 0.78 mg m^{-3}) and not detectable deeper
400 than 150 m depth. The OBS signal showed a distinct zone of enhanced turbidity on the continental
401 margin between 200-350 m water depth.



402

403 **Figure 7** CTD transect across the Angolan margin. Shown are data for (a) potential temperature ($^{\circ}\text{C}$), (b) salinity (PSU), (c)
 404 dissolved oxygen concentration (ml l^{-1}), (d) fluorescence (mg m^{-3}), (e) turbidity (NTU) (data plotted using Ocean Data View
 405 v.4.7.8; <http://odv.awi.de>; Schlitzer, 2011). The depth occurrence of CWC mounds is marked by a red, dashed line, the lander
 406 deployments are indicated by colored dots.

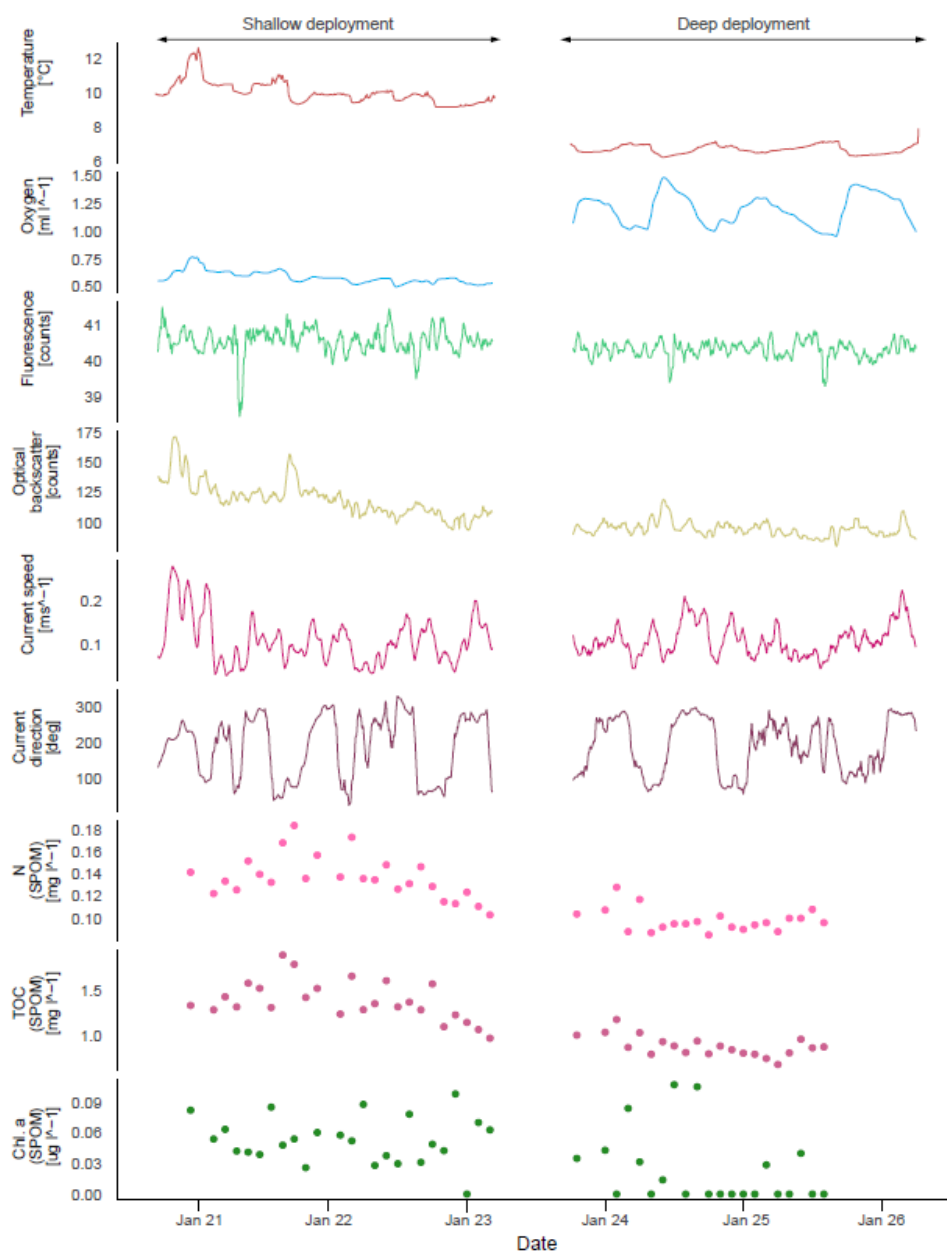
407 3.2.2 Lander time series physical data

408 Mean bottom water temperatures varied from the deepest to the shallowest site between 6.73–10.06 $^{\circ}\text{C}$
 409 (Fig. 8). The maximum semidiurnal ($\Delta t \sim 6\text{h}$) temperature change varied between 0.82 to 1.60 $^{\circ}\text{C}$ at the
 410 deepest and shallowest site respectively. At the shallow site, the maximum short-term temperature
 411 change was 2.4 $^{\circ}\text{C}$ (Fig. 8). DO_{conc} at the deep site were a factor of two higher than those at the shallow
 412 site, i.e. 0.9–1.5 vs. 0.5–0.8 ml l^{-1} respectively (\cong range between 4–14% saturation of both sites), where
 413 also the range of diurnal fluctuations was much smaller compared to the shallow site. DO_{conc} were
 414 negatively correlated with temperature at the deep site ($r=-0.99$, $p<0.01$) while positively correlated at
 415 the shallow site ($r=0.91$, $p<0.01$). Fluorescence was overall low during both deployments and showed
 416 only small fluctuations whereas it was slightly higher at the shallow site (between 38.5 and 41.5 NTU at
 417 both sites). Current speeds were relatively high (between 0–0.3 m s^{-1} , average 0.1 m s^{-1}) and positively



418 correlated with temperature at the shallow site ($r=0.31$, $p<0.01$) and negatively correlated at the deep
419 site ($r=-0.22$, $p<0.01$). Analysis of the tidal cycle showed, that it explains 29.8-54.9% of the horizontal
420 current fluctuations. The M2 (principal lunar semi-diurnal) amplitude was 0.06-0.09 m s^{-1} and was the
421 most important signal (Table 2). The OBS measurements showed a decreasing turbidity during the
422 deployment at the shallow station. This station was located directly below the turbidity maximum
423 between 200-350 m depth as observed in the CTD transect (Fig.7). In contrast, a relative constant and
424 low turbidity was observed for the deep deployment. Turbidity during both deployments was positively
425 correlated to DO_{conc} ($r=0.47$, $p<0.01$, shallow and $r=0.50$, $p<0.01$, deep). The SLM lander was deployed at
426 a depth of 440 m and recorded an average pH of 8.12.

427 The short-term temperature fluctuations imply a vertical tidal movement of around 130 m, based on
428 comparing the temperature range measured by the lander and the temperature versus depth gradient
429 based on CTD measurements (12.9-9.1 °C measured by lander \triangleq 218-349 m depth in CTD above lander
430 at station GeoB20966).



431

432 **Figure 8** Lander data (ALBEX) recorded during the shallow (~340 m water depth) and deep deployments (~530 m water depth)
 433 off Angola (January 2016). Shown are temperature (°C; red), dissolved oxygen concentration (ml l⁻¹; blue), fluorescence (counts
 434 per second; green), optical backscatter (turbidity; yellow), current speed (m s⁻¹; pink) and current direction (degree: 0-360°;
 435 purple) as well as nitrogen (mg l⁻¹; pink dots), carbon (mg l⁻¹; purple dots), and chlorophyll-α concentration (µg l⁻¹; green dots) of
 436 SPOM collected during the both deployments by the McLane pump.



437 3.2.3 Food supply

438 In general TOC and N concentrations of SPOM measured on the filters from the McLane pump were
439 lower at the deep site. Nitrogen concentrations varied around 0.14 mg l^{-1} at 342 m and around 0.1 mg l^{-1}
440 at 532 m depth (Fig. 6b). The $\delta^{15}\text{N}$ values of the lander time series of the shallow deployment ranged
441 from 1.6 to 6.2 ‰ (3.7 ‰ average) and were even lower deeper in the water column, viz. range 0.3-3.7
442 ‰ with an average of 1.4 ‰. The TOC concentrations were on average 1.43 mg l^{-1} at 342 m and 0.9 mg l^{-1}
443 at 532 m, with corresponding $\delta^{13}\text{C}$ values ranging between -23.0 and -24.2 (average of -23.6 ‰) at the
444 shallow and between -22.9 and -23.9 (average -23.4 ‰) at the deep site. The C/N ratio was relatively
445 stable and on average 10.2 and 9 for the samples taken at the shallower and deeper site, respectively.

446 The chlorophyll- α concentrations of the SPOM collected by the McLane pump varied between 0.1 and
447 $0.02 \mu\text{g l}^{-1}$, with an average phaeopigments/chlorophyll- α ratio of 2.6 and 0.5 on the shallow and deep
448 site, respectively. Phytopigments recorded by the shallow deployment included $0.3 \mu\text{g l}^{-1}$ of fucoxanthin,
449 while at the deep site only a concentration of $0.1 \mu\text{g l}^{-1}$ was found. No zeaxanthin was recorded in the
450 pigment fraction.

451 4. Discussion

452 Even though the ecological-niche factor analysis of Davies et al. (2008) and Davies and Guinotte (2011)
453 predict *L. pertusa* to be absent on the oxygen-limited southwestern African margin, two CWC mound
454 ecosystems were observed along the Namibian and Angolan margins. The coral mounds on the Namibian
455 shelf host no living CWCs, instead dead coral framework covering the mounds was overgrown with fauna
456 dominated by bryozoans and sponges. Along the slope of the Angolan margin an extended coral mound
457 area with thriving CWC communities was encountered. Differences between the areas indicate different
458 environmental conditions influencing faunal assemblages present in both areas. The potential impact of
459 the key environmental factors will be discussed below.

460 4.1 Short-term vs long-term variations in environmental properties

461 On the Namibian margin, seasonality has a major impact on local-mid-depth oxygen concentration due
462 to the periodically varying influence of the Angola current and its associated low DO_{conc} . The lowest
463 DO_{conc} are expected from February to May when SACW is the dominating water mass on the Namibian
464 margin and the contribution of ESAC water is smaller. Due to this seasonal pattern, the DO_{conc} measured
465 in this study (January; Figs. 4) most likely do not represent minimum concentrations, which are expected
466 to occur in the following months (February to May; Mohrholz et al., 2014). Interestingly, we captured a
467 flow reversal from a southward to an equatorward current direction during high wind conditions on the



468 Namibian margin (Fig. 5), leading to an intrusion of ESACW with higher DO_{conc} (+0.007 ml l⁻¹ on average)
469 and lower temperatures (-0.23°C on average, Fig. 5) than the SACW after the 6th of January, leading to
470 an temporal relaxation of the oxygen stress. This shows that variations in the local flow field have the
471 capability to change water properties on relatively short time scales, which might provide an analogue
472 to the water mass variability related to the different seasons. Such relaxations are likely important for
473 the survival of the abundant invertebrate fauna present on the relict coral mounds under the conditions
474 generally considered unsuited for them. Other seasonal changes, like riverine outflow do not have
475 decisive impacts on the margin ecosystem since only relatively small rivers discharge from the Namibian
476 margin. This is also reflected by the dominant marine isotopic signature of the isotopic ratios of $\delta^{15}N$ and
477 $\delta^{13}C$ of the suspended particulate matter at the mound areas (Fig. 6, cf. Tyrrell and Lucas, 2002).

478 Flow reversals were not observed during the lander deployments on the Angolan margin, where winds
479 are reported to be weak throughout the year providing more stable conditions (Shannon, 2001). Instead
480 river outflow seems to exert a strong influence on the oxygen concentration on the Angolan margin. The
481 run-off of the Cuanza and Congo river reach their seasonal maximum in December and January (Kopte et
482 al., 2017), intensifying upper water column stratification and transporting terrestrial organic matter to
483 the margin. This stratification is restricting vertical mixing and thereby limits ventilation of the oxygen
484 depleted subsurface water masses. The input of terrestrial organic matter is reflected by the isotopic
485 signals of the SPOM, i.e. a $\delta^{15}N$ values between 1.4 to 3.7‰. This range resembles a more terrestrial
486 signal (-1 to 3‰; Montoya, 2007) and is well below the average isotopic ratio of the marine waters of
487 5.5‰ (Meisel et al., 2011). Also $\delta^{13}C$ values of -23.5‰ are in line with the $\delta^{13}C$ values of terrestrial
488 matter which is on average -27 ‰ in this area (Boutton, 1991; Mariotti et al., 1991). The C/N ratio of
489 SPOM is higher compared to material from the Namibian margin, confirming admixing of terrestrial
490 matter (Perdue and Koprivnjak, 2007). The combined effects of decreased vertical mixing and additional
491 input of organic matter potentially result in the lowest DO_{conc} of the year during the investigated time
492 period (January), since the highest river outflow and therefore strongest stratification is expected during
493 this period.

494 *4.2 Main stressors – Oxygen and temperature*

495 Environmental conditions marked by severe hypoxia and temporal anoxia (<0.17 ml l⁻¹) likely explain the
496 present-day absence of living CWCs along the Namibian margin. During the measurement period the
497 DO_{conc} off Namibia were considerably lower than the thus far recorded minimum concentrations near
498 living CWCs (1-1.3 ml l⁻¹), which were found off Mauritania where only isolated living CWCs are found



499 (Ramos et al., 2017). Age dating of the Namibian fossil coral framework shows that CWCs disappeared
500 about 5 ka BP, which coincides with an intensification in upwelling and therefore most likely a decline of
501 DO_{conc} (Tamborrino et al., submitted). This is supporting the assumption that the DO_{conc} is responsible for
502 the demise of CWCs on the Namibian margin. Although no living corals were observed on the Namibian
503 coral mounds, we observed a dense living community dominated by sponges and bryozoans (Hebbeln et
504 al., 2017). Several sponge species have been reported to survive at extremely low DO_{conc} within OMZs.
505 For instance, along the lower boundary of the Peruvian OMZ sponges were found at DO_{conc} as low as
506 $0.06\text{--}0.18\text{ ml l}^{-1}$ (Mosch et al., 2012). Mills et al. (2018) recently found a sponge (*Tethya wilhelma*) to be
507 physiologically almost insensitive to oxygen stress and to respire aerobically under low DO_{conc} (0.02 ml l^{-1}
508). Sponges can potentially stop their metabolic activity during unfavorable conditions and re-start their
509 metabolism when some oxygen becomes available, for instance during diurnal irrigation of water with
510 somewhat higher DO_{conc} . The existence of a living sponge community off Namibia might hence be
511 explained by the diurnal baroclinic tides occasionally flushing the sponges with more oxic water enabling
512 them to metabolize, when food availability is also highest (pulse of suspended particulate matter with a
513 higher amount of TOC and N during oxygenated conditions, Figs. 5, 8). Increased biomass and
514 abundances in these temporary hypoxic-anoxic transition zones were already observed for macro- and
515 mega-fauna in other OMZs and is referred to as the “edge effect” (Mullins et al., 1985; Levin et al.,
516 1991; Sanders, 1969). It is very likely that this mechanism plays a role for the benthic communities on the
517 Angolan margin.

518 Along the Angolan margin low oxygen concentrations apparently do not restrict the proliferation of
519 thriving CWC reefs even though DO_{conc} are considered hypoxic ($0.5\text{--}1.5\text{ ml l}^{-1}$). The DO_{conc} measured off
520 Angola are well below the lower DO_{conc} limits for *L. pertusa* based either on habitat suitability modelling
521 (Davies et al., 2008) or on laboratory experiments and earlier field observations (Schroeder, 2002; Brooke
522 and Ross, 2014). The DO_{conc} encountered at the shallow mound sites ($<0.8\text{ ml l}^{-1}$) are even below the so far
523 lowest limits known for single CWC colonies from the Mauritanian margin (Ramos et al., 2017b). Since in
524 the present study, measured DO_{conc} were even lower than the earlier established lower limits³ this could
525 suggest a much higher tolerance of *L. pertusa* to low oxygen levels at least in a limited time-period as
526 low as 0.5 ml l^{-1} (4% O_2 saturation), which was measured by the ALBEX lander as well as the CTD during
527 the cruise in 2016. Even though concentrations at the Angolan margin showed to be relatively stable, it
528 should be emphasized that the observation period was limited and long-term (year-long) observations
529 remain necessary to confidently extend the lower limit of oxygen deficiency tolerance by *L. pertusa*.



530 In addition to the oxygen stress, heat stress is expected to put additional pressure on CWCs. Temperatures
531 at the CWC mounds off Angola ranged from 6.4 to 12.6 °C, which are close to their reported maximum
532 temperatures (~12-14.9 °C; Davies and Guinotte 2011) and are hence expected to impair the ability of
533 CWCs to form mounds (see Wienberg and Titschack 2017). In most aquatic invertebrates respiration rates
534 roughly double with every 10 °C increase (Q_{10} temperature coefficient = 2-3, e.g. Coma 2002), which at
535 the same time doubles energy demand. Dodds et al. (2007) found a doubling of the respiration rate of *L.*
536 *pertusa* with an increase at ambient temperature of only 2 °C (viz. $Q_{10}=7-8$). This would limit the survival
537 of *L. pertusa* at high temperatures to areas where the increased demand in energy (due to increased
538 respiration) can be compensated by high food availability. Higher respiration rates also imply that enough
539 oxygen needs to be available for the increased respiration.

540 Survival of *L. pertusa* under hypoxic conditions along the shallow Angolan CWC areas is probably positively
541 influenced by the fact that periods of highest temperatures coincide with highest DO_{conc} during the tidal
542 cycle, which stands in contrast to mounds on the Namibian margin or the deeper Angolan mound area.
543 Probably the increase of one stressor is compensated by a reduction of another stressor in the shallow
544 Angolan mound areas. On the Namibian margin or the deeper Angolan mound sites we found the opposite
545 pattern, with highest temperatures during lowest DO_{conc} . The occurrence of *L. pertusa* at the the deeper
546 Angolan mound sites is possibly related to the fact that DO_{conc} are anyway higher and temperatures more
547 within a suitable range compared to the shallow sites (0.9-1.5 ml l⁻¹, 6.4-8 °C, Fig. 8). Additionally it was
548 shown by ex situ experiments that *L. pertusa* is able to survive periods of hypoxic conditions similar to
549 those found along the Angolan margin for several days, which could be crucial in periods of most adverse
550 conditions during one tidal period or also slightly longer time periods (Dodds et al., 2007). However,
551 oxygen stress leads to a loss of energy which and associated increased energy demand like in other aquatic
552 invertebrates (Sokolova et al., 2012).

553 *4.3 Food supply*

554 As mentioned above, environmental stress like high temperature or low DO_{conc} result in a loss of energy
555 (Odum, 1971; Sokolova et al., 2012), which needs to be balanced by an increased energy (food) availability.
556 Food availability therefore plays a significant role for faunal abundance under hypoxia or unfavorable
557 temperatures (Diaz and Rosenberg, 1995). Above, we argued that survival of sponges and bryozoans on
558 the relict mounds off Namibia and of CWCs and their associated fauna at the Angolan margin, may be
559 partly due to a high input of high-quality organic matter, compensating the oxygen and thermal stresses.
560 The importance of the food availability for CWCs was already suggested by Eisele et al. (2011), who



561 mechanistically linked CWC mound growth periods with enhanced surface water productivity and hence
562 organic matter supply. Here we found evidence for high quality and quantity of SPOM in the vicinity of
563 the coral mounds on the Namibian as well as on the Angolan margin. Indicators for the high quality of
564 food in the SPOM at both sites were high TOC and N concentrations (Figs. 6, 10) in combination with a
565 low C/N ratio (Fig. 7), a low isotopic signature of $\delta^{15}\text{N}$ and only slightly degraded pigments
566 ($\Sigma\text{phaeopigment}/\text{chlorophyll-}\alpha$ ratio of on average 6.5 and 3.2 off Namibia and Angola, respectively).

567 The Namibian margin is known for its upwelling cells, where phytoplankton growth is fueled by nutrients
568 from deeper water layers producing high amounts of phytodetritus (Chapman and Shannon, 1985), which
569 subsequently sinks down to the relict mounds on the slope. This high flux and accumulation of fresh SPOM
570 towards the reefs is evident as a slightly increased fluorescence deeper in the water column around the
571 mound sites (Fig. 4d). Furthermore, the increased fluorescence and chlorophyll- α concentrations coincide
572 with low DO_{conc} which both are in line with downward movement of waters with a lower DO_{conc} from the
573 OMZ above (Fig. 5). The higher turbidity during lower current speeds provides additional evidence that
574 the material settling from the surface is not transported away with the strong currents (Fig. 5). Mounds
575 off Namibia occur at relatively shallow depths, hence downward transport of SPOM from the surface
576 waters is rapid and hence time for decomposition of the sinking particles in the water column is limited.
577 This fast delivery of SPOM over short depth intervals appears to be linked to both, high primary
578 productivity (high surface fluorescence, Fig. 4d) and reduced decomposition due to low oxygen
579 concentrations (Pichevin et al., 2004; Cavan et al., 2017), leads to a generous food supply for several
580 benthic organisms thus enabling them to survive under hypoxic conditions.

581 At the Angolan coral mounds, SPOM appeared to have a signature corresponding to higher quality organic
582 matter compared to off Namibia. The phytopigments were less degraded (i.e. higher chlorophyll- α
583 concentration, lower $\Sigma\text{phaeopigment}/\text{chlorophyll-}\alpha$ ratio) and the $\delta^{15}\text{N}$, TOC and N concentration of the
584 SPOM was lower than off Namibia. However, here lower $\delta^{15}\text{N}$ and higher $\Sigma\text{phaeopigment}/\text{chlorophyll-}\alpha$
585 ratio are likely connected to terrestrial OM input, which constitutes a less suitable food source for CWCs.
586 On the other hand the riverine input delivers nutrients, which can support the growth of phytoplankton,
587 indirectly influencing food supply (Kiriakoulakis et al., 2007; Mienis et al., 2012). Moreover the food quality
588 at the shallow Angolan reefs was not coupled to periods of other environmental stressors and variations
589 were relatively small during this study. At the Angolan margin we see a rather constant delivery of SPOM.
590 The slightly higher turbidity during periods of highest DO_{conc} , (Fig. 8) suggest that the SPOM on the Angolan
591 margin originates from the bottom nepheloid layer on the margin directly above the CWC mounds (Fig.

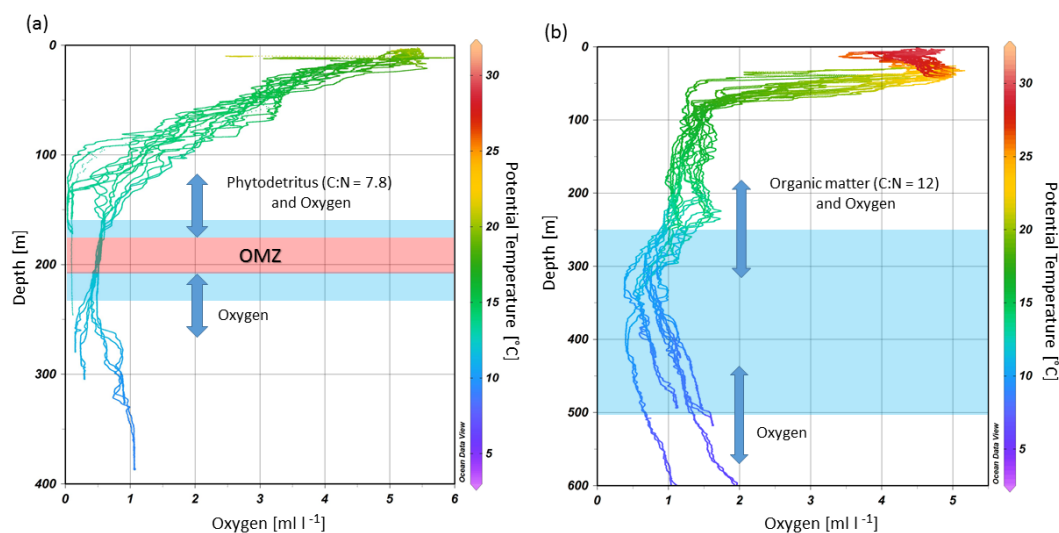


592 7e), which may represent a constant reservoir of fresh SPOM. This again indicates that CWCs can benefit
593 from a constant source of high quality SPOM on the margin somewhat above the coral mound areas and
594 are not exclusively depending on SPOM settling from the surface (like at the Namibian margin), since the
595 strong stratification inhibits mixing of the different water masses. This is also supported by the fact, that's
596 increased fluorescence off Angola was not as strongly correlated with the downward currents as off
597 Namibia.

598 *4.4 Tidal currents*

599 The semidiurnal tidal currents observed probably play a major role in the survival of benthic fauna on the
600 southwestern African margin. On the Namibian margin internal waves deliver oxygen from the surface
601 and deeper waters semi-diurnally about 70 m towards to the inside the OMZ and thereby enable benthic
602 fauna on the fossil coral framework to survive in hypoxic conditions (Fig. 9a). At the same time these
603 currents are likely responsible for the delivery of fresh SPOM from the surface productive zone to the
604 communities on the margin.

605 On the Angolan margin internal tides produce slightly faster currents and vertical excursions of up to 130
606 m which are twice as high as those on the Namibian margin. Similar to the Namibian margin these tidal
607 excursions deliver oxygen from shallower and deeper waters to the mound zone (Fig. 9b). Internal tides
608 are also responsible for the formation of a bottom nepheloid layer in 200-350 m depth (Fig. 7e). This layer
609 is formed by bottom erosion due to the intensification of near-bottom water movements, which is
610 indicated by maxima of the buoyancy frequency N^2 in 225 and 300 m depth (GeoB20977-1, not shown).
611 Tidal waves will be amplified due to a critical match between the characteristic slope of the internal M2
612 tide and the bottom slope of the Angolan margin, as is known from other continental slope regions
613 (Dickson and McCave, 1986; Mienis et al., 2007). As argued above, this turbid layer is likely important for
614 the nutrition of the slightly deeper situated CWC mounds, since vertical mixing is hindered by the strong
615 stratification.



616

617 **Figure 9** Depth range of cold-water coral mound occurrences (blue shaded areas) at the (a) Namibian and (b) Angolan margins
618 in relation to the dissolved oxygen concentrations and potential temperature. Diurnal tides are delivering mainly phytodetritus
619 (shown in (a)) and organic matter from the benthic nepheloid layer (shown in (b)) as well as oxygen from above, and from below
620 to the mound sites (indicated by blue arrows, the length of which indicate the tidal ranges).

621 **4.5 Implications**

622 CWC and sponge communities are known to play an important role as a refuge, feeding ground and
623 nursery for commercial fishes (Miller et al., 2012) and have a crucial role in the marine benthic pelagic
624 coupling (Cathalot et al., 2015). CWCs and their ecosystem services are threatened by the expected
625 expansion of OMZs due to anthropogenic activities like rising nutrient loads and climate change
626 (Breitburg et al., 2018). This study showed that CWCs are able to cope with low oxygen levels as long as
627 sufficient high quality food is available. Further, reef associated sponge grounds, as encountered on the
628 Namibian margin could play a crucial role in taking over the function of CWCs in marine carbon cycling
629 as well as in providing a habitat for associated fauna, when conditions become unsuitable for CWCs.

630 **5. Conclusions**

631 Different environmental properties and different relations between these properties explain the
632 dissimilar present conditions of CWCs on the southwestern African margin including temperature,
633 DO_{conc} , food supply and tidal movements. The DO_{conc} likely defines the state of the CWCs along the
634 Namibian and the Angolan margin, whereas high temperatures constitute an additional stressor by
635 increasing the respiration rate and therefore energy demand. On the Namibian margin, where DO_{conc}



636 dropped below 0.01 ml l^{-1} , only fossil CWC mounds covered by a community dominated by sponges and
637 bryozoans were found. This community survives as it receives periodically waters with slightly higher
638 DO_{conc} ($>0.03 \text{ ml l}^{-1}$) due to regular tidal oscillations (semi diurnal) and erratic wind events (seasonal). At
639 the same time, a high quality and quantity of SPOM sinking down from the surface water mass enables
640 the epifaunal community to survive despite the oxygen stress and sustain its metabolic energy demand
641 at the Namibian OMZ, while CWCs are not capable to withstand such extreme conditions. In contrast,
642 thriving CWCs on the Angolan coral mounds were encountered despite the overall hypoxic conditions.
643 The DO_{conc} were slightly higher than those on the Namibian margin, but nevertheless below the lowest
644 threshold that was so far reported for *L. pertusa* (Ramos et al., 2017; Davies et al., 2010; Davies et al.,
645 2008). In combination with temperatures, close to the upper limits for *L. pertusa*, metabolic energy
646 demand probably reached a maximum. High energy requirements might have been compensated by the
647 general high availability of fresh resuspended SPOM. Fresh SPOM is accumulated on the Angolan margin
648 just above the CWC area and is regularly supplied due to mixing by semidiurnal tidal currents, despite
649 the restricted sinking of SPOM from the surface due to the strong stratification.

650 6. Data availability

651 Data will be uploaded to Pangea after publication.

652

653 7. Author contribution

654 UH analyzed the physical and chemical data, wrote the manuscript and prepared the figures with
655 contributions of all authors. FM, GD and ML designed the lander research. DH and CW led the cruise and
656 wrote the initial cruise plan. FM and ML collected the data during the research cruise. WCD was
657 responsible for water column measurements with the CTD. AF and ML provided habitat characteristics,
658 including species identification of both CWC areas. KJ performed the tidal analysis and provided
659 together with SF data of the SML lander. All authors contributed to the data interpretation and
660 discussion of the manuscript.

661

662 8. Competing interests

663 The authors declare that they have no conflict of interest.

664



665 9. Acknowledgements

666 We thank the Captain of the RV *Meteor* cruise M122, Rainer Hammacher, his officers and crew, which
667 contributed to the success of this cruise. We also like to thank the scientific and technical staff for their
668 assistance during the cruise and the work in the laboratory. Greatly acknowledged are the efforts from
669 the German Diplomatic Corps in the German Embassies in Windhoek and Luanda and in the Foreign
670 Office in Berlin. We thank the German Science Foundation (DFG) for providing ship time on RV *Meteor*
671 and for funding the ROV *Squid* operations to investigate the cold-water coral ecosystems off Angola and
672 Namibia. This work was further supported through the DFG Research Center/ Cluster of Excellence
673 “MARUM – The Ocean in the Earth System”. UH is funded by the SponGES project, which received
674 funding from the European Union's Horizon 2020 research and innovation program under grant
675 agreement No 679849. FM is supported by the Innovational Research Incentives Scheme of the
676 Netherlands Organisation for Scientific Research (NWO-VIDI grant 016.161.360). GJR is supported by the
677 Netherlands Earth System Science Centre (NESSC), financially supported by the Ministry of Education,
678 Culture and Science (OCW). We also thank the Norwegian Research Council (NRC) for funding. KJ is
679 funded through the FATE project (Fate of cold-water coral reefs – identifying drivers of ecosystem
680 change).

681 10. References

- 682 Boutton, T. W.: Stable carbon isotope ratios of natural materials: II. Atmospheric, terrestrial, marine, and
683 freshwater environments, *Carbon isotope techniques*, 1, 173, 1991.
- 684 Breitburg, D., Levin, L. A., Oschlies, A., Grégoire, M., Chavez, F. P., Conley, D. J., Garçon, V., Gilbert, D.,
685 Gutiérrez, D., and Isensee, K.: Declining oxygen in the global ocean and coastal waters, *Science*, 359,
686 eaam7240, 2018.
- 687 Brooke, S., and Ross, S. W.: First observations of the cold-water coral *Lophelia pertusa* in mid-Atlantic
688 canyons of the USA, *Deep Sea Research Part II: Topical Studies in Oceanography*, 104, 245-251, 2014.
- 689 Buhl-Mortensen, L., Vanreusel, A., Gooday, A. J., Levin, L. A., Priede, I. G., Buhl-Mortensen, P.,
690 Gheerardyn, H., King, N. J., and Raes, M.: Biological structures as a source of habitat heterogeneity and
691 biodiversity on the deep ocean margins, *Marine Ecology*, 31, 21-50, 2010.
- 692 Cairns, S. D.: Deep-water corals: an overview with special reference to diversity and distribution of deep-
693 water scleractinian corals, *Bulletin of Marine Science*, 81, 311-322, 2007.
- 694 Carr, M.-E., and Kearns, E. J.: Production regimes in four Eastern Boundary Current systems, *Deep Sea*
695 *Research Part II: Topical Studies in Oceanography*, 50, 3199-3221, 2003.
- 696 Cathalot, C., Van Oevelen, D., Cox, T. J., Kutti, T., Lavaleye, M., Duineveld, G., and Meysman, F. J.: Cold-
697 water coral reefs and adjacent sponge grounds: Hotspots of benthic respiration and organic carbon
698 cycling in the deep sea, *Frontiers in Marine Science*, 2, 37, 2015.
- 699 Cavan, E. L., Trimmer, M., Shelley, F., and Sanders, R.: Remineralization of particulate organic carbon in
700 an ocean oxygen minimum zone, *Nature communications*, 8, 14847, 2017.
- 701 Chapman, P., and Shannon, L.: The Benguela ecosystem, Part II. Chemistry and related processes.
702 *Oceanography and Marine Biology. An Annual Review*, 23, 183-251, 1985.



- 703 Chapman, P., and Shannon, L.: Seasonality in the oxygen minimum layers at the extremities of the
704 Benguela system, *South African Journal of Marine Science*, 5, 85-94, 1987.
- 705 Coma, R.: Seasonality of in situ respiration rate in three temperate benthic suspension feeders,
706 *Limnology and Oceanography*, 47, 324-331, 2002.
- 707 Costello, M. J., McCrea, M., Freiwald, A., Lundälv, T., Jonsson, L., Bett, B. J., van Weering, T. C., de Haas,
708 H., Roberts, J. M., and Allen, D.: Role of cold-water *Lophelia pertusa* coral reefs as fish habitat in the NE
709 Atlantic, in: *Cold-water corals and ecosystems*, Springer, Heidelberg, 771-805, 2005.
- 710 Davies, A. J., Wisshak, M., Orr, J. C., and Roberts, J. M.: Predicting suitable habitat for the cold-water
711 coral *Lophelia pertusa* (Scleractinia), *Deep Sea Research Part I: Oceanographic Research Papers*, 55,
712 1048-1062, 2008.
- 713 Davies, A. J., Duineveld, G. C., Lavaleye, M. S., Bergman, M. J., van Haren, H., and Roberts, J. M.:
714 Downwelling and deep-water bottom currents as food supply mechanisms to the cold-water coral
715 *Lophelia pertusa* (Scleractinia) at the Mingulay Reef Complex, *Limnology and Oceanography*, 54, 620-
716 629, 2009.
- 717 Davies, A. J., Duineveld, G. C., van Weering, T. C., Mienis, F., Quattrini, A. M., Seim, H. E., Bane, J. M., and
718 Ross, S. W.: Short-term environmental variability in cold-water coral habitat at Viosca Knoll, Gulf of
719 Mexico, *Deep Sea Research Part I: Oceanographic Research Papers*, 57, 199-212, 2010.
- 720 Davies, A. J., and Guinotte, J. M.: Global habitat suitability for framework-forming cold-water corals, *PloS*
721 *one*, 6, e18483, 2011.
- 722 De Haas, H., Mienis, F., Frank, N., Richter, T. O., Steinacher, R., De Stigter, H., Van der Land, C., and Van
723 Weering, T. C.: Morphology and sedimentology of (clustered) cold-water coral mounds at the south
724 Rockall Trough margins, NE Atlantic Ocean, *Facies*, 55, 1-26, 2009.
- 725 Diaz, R. J., and Rosenberg, R.: Marine benthic hypoxia: a review of its ecological effects and the
726 behavioural responses of benthic macrofauna, *Oceanography and Marine Biology. An Annual Review*,
727 33, 245-203, 1995.
- 728 Dickson, R., and McCave, I.: Nepheloid layers on the continental slope west of Porcupine Bank, *Deep Sea*
729 *Research Part A. Oceanographic Research Papers*, 33, 791-818, 1986.
- 730 Dodds, L., Roberts, J., Taylor, A., and Marubini, F.: Metabolic tolerance of the cold-water coral *Lophelia*
731 *pertusa* (Scleractinia) to temperature and dissolved oxygen change, *Journal of Experimental Marine*
732 *Biology and Ecology*, 349, 205-214, 2007.
- 733 Dodds, L., Black, K., Orr, H., and Roberts, J.: Lipid biomarkers reveal geographical differences in food
734 supply to the cold-water coral *Lophelia pertusa* (Scleractinia), *Marine Ecology Progress Series*, 397, 113-
735 124, 2009.
- 736 Duineveld, G. C., Lavaleye, M. S., Bergman, M. J., De Stigter, H., and Mienis, F.: Trophic structure of a
737 cold-water coral mound community (Rockall Bank, NE Atlantic) in relation to the near-bottom particle
738 supply and current regime, *Bulletin of Marine Science*, 81, 449-467, 2007.
- 739 Dullo, W.-C., Flögel, S., and Rüggeberg, A.: Cold-water coral growth in relation to the hydrography of the
740 Celtic and Nordic European continental margin, *Marine Ecology Progress Series*, 371, 165-176, 2008.
- 741 Eisele, M., Frank, N., Wienberg, C., Hebbeln, D., Correa, M. L., Douville, E., and Freiwald, A.: Productivity
742 controlled cold-water coral growth periods during the last glacial off Mauritania, *Marine Geology*, 280,
743 143-149, 2011.
- 744 Fink, H. G., Wienberg, C., Hebbeln, D., McGregor, H. V., Schmiel, G., Taviani, M., and Freiwald, A.:
745 Oxygen control on Holocene cold-water coral development in the eastern Mediterranean Sea, *Deep Sea*
746 *Research Part I: Oceanographic Research Papers*, 62, 89-96, 2012.
- 747 Flögel, S., Dullo, W.-C., Pfannkuche, O., Kiriakoulakis, K., and Rüggeberg, A.: Geochemical and physical
748 constraints for the occurrence of living cold-water corals, *Deep Sea Research Part II: Topical Studies in*
749 *Oceanography*, 99, 19-26, 2014.



- 750 Frederiksen, R., Jensen, A., and Westerberg, H.: The distribution of the scleractinian coral *Lophelia*
751 *pertusa* around the Faroe Islands and the relation to internal tidal mixing, *Sarsia*, 77, 157-171, 1992.
- 752 Freiwald, A.: Reef-forming cold-water corals, in: *Ocean margin systems*, Springer, 365-385, 2002.
- 753 Freiwald, A., Fossa, J. H., Grehan, A., Koslow, T., and Roberts, J. M.: Cold water coral reefs: out of sight-
754 no longer out of mind, 2004.
- 755 Freiwald, A., Beuck, L., Rüggeberg, A., Taviani, M., Hebbeln, D., and Participants, R. V. M. C. M.-. The
756 white coral community in the central Mediterranean Sea revealed by ROV surveys, *Oceanography*, 22,
757 58-74, 2009.
- 758 Geissler, W., Schwenk, T., and Wintersteller, P.: Walvis Ridge Passive-Source Seismic Experiment
759 (WALPASS) – Cruise No. MSM20/1 – January 06 – January 15, 2012 - Cape Town (South Africa) – Walvis
760 Bay (Namibia), DFG-Senatskommission für Ozeanographie, MARIA S. MERIAN-Berichte, MSM20/1, 54
761 pp., 2013.
- 762 Gori, A., Grover, R., Orejas, C., Sikorski, S., and Ferrier-Pagès, C.: Uptake of dissolved free amino acids by
763 four cold-water coral species from the Mediterranean Sea, *Deep Sea Research Part II: Topical Studies in*
764 *Oceanography*, 99, 42-50, 2014.
- 765 Grasmueck, M., Eberli, G. P., Viggiano, D. A., Correa, T., Rathwell, G., and Luo, J.: Autonomous
766 underwater vehicle (AUV) mapping reveals coral mound distribution, morphology, and oceanography in
767 deep water of the Straits of Florida, *Geophysical Research Letters*, 33, 2006.
- 768 Hebbeln, D., Wienberg, C., Wintersteller, P., Freiwald, A., Becker, M., Beuck, L., Dullo, W.-C., Eberli, G.,
769 Glogowski, S., and Matos, L.: Environmental forcing of the Campeche cold-water coral province,
770 southern Gulf of Mexico, *Biogeosciences* (BG), 11, 1799-1815, 2014.
- 771 Hebbeln, D., Wienberg, C., Bender, M., Bergmann, F., Dehning, K., Dullo, W.-C., Eichstädter, R., Flöter, S.,
772 Freiwald, A., Gori, A., Haberkern, J., Hoffmann, L., João, F., Lavaleye, M., Leymann, T., Matsuyama, K.,
773 Meyer-Schack, B., Mienis, F., Moçambique, I., Nowald, N., Orejas, C., Ramos Cordova, C., Saturov, D.,
774 Seiter, C., Titschack, J., Vittori, V., Wefing, A.-M., Wilsenack, M., and Wintersteller, P.: ANNA Cold-Water
775 Coral Ecosystems off Angola and Namibia - Cruise No. M122 - December 30, 2015 - January 31, 2016 -
776 Walvis Bay (Namibia) - Walvis Bay (Namibia), *METEOR-Berichte*, M122 https://doi.org/10.2312/cr_m122
777 2017.
- 778 Henry, L.-A., and Roberts, J. M.: Biodiversity and ecological composition of macrobenthos on cold-water
779 coral mounds and adjacent off-mound habitat in the bathyal Porcupine Seabight, NE Atlantic, *Deep Sea*
780 *Research Part I: Oceanographic Research Papers*, 54, 654-672, 2007.
- 781 Henry, L.-A., and Roberts, J. M.: Global Biodiversity in Cold-Water Coral Reef Ecosystems, in: *Marine*
782 *Animal Forests*, Springer, 235-256, 2017.
- 783 Junker, T., Mohrholz, V., Siegfried, L., and van der Plas, A.: Seasonal to interannual variability of water
784 mass characteristics and currents on the Namibian shelf, *Journal of Marine Systems*, 165, 36-46, 2017.
- 785 Karstensen, J., Stramma, L., and Visbeck, M.: Oxygen minimum zones in the eastern tropical Atlantic and
786 Pacific oceans, *Progress in Oceanography*, 77, 331-350, 2008.
- 787 Kiriakoulakis, K., Fisher, E., Wolff, G. A., Freiwald, A., Grehan, A., and Roberts, J. M.: Lipids and nitrogen
788 isotopes of two deep-water corals from the North-East Atlantic: initial results and implications for their
789 nutrition, in: *Cold-water corals and ecosystems*, edited by: Freiwald, A. a. R., J.M. (eds.), Springer,
790 Heidelberg, 715-729, 2005.
- 791 Kiriakoulakis, K., Freiwald, A., Fisher, E., and Wolff, G.: Organic matter quality and supply to deep-water
792 coral/mound systems of the NW European Continental Margin, *International Journal of Earth Sciences*,
793 96, 159-170, 2007.
- 794 Kopte, R., Brandt, P., Dengler, M., Tchikalanga, P., Macuéria, M., and Ostrowski, M.: The Angola Current:
795 Flow and hydrographic characteristics as observed at 11° S, *Journal of Geophysical Research: Oceans*,
796 122, 1177-1189, 2017.



- 797 Kostianoy, A., and Lutjeharms, J.: Atmospheric effects in the Angola-Benguela frontal zone, *Journal of*
798 *Geophysical Research: Oceans*, 104, 20963-20970, 1999.
- 799 Kraay, G. W., Zapata, M., and Veldhuis, M. J.: Separation of Chlorophylls c1c2, and c3 of marine
800 Phytoplankton by Reverse Phase C18 high Performance liquid Chromatography 1, *Journal of Phycology*,
801 28, 708-712, 1992.
- 802 Le Guilloux, E., Olu, K., Bourillet, J.-F., Savoye, B., Iglésias, S., and Sibuet, M.: First observations of deep-
803 sea coral reefs along the Angola margin, *Deep Sea Research Part II: Topical Studies in Oceanography*, 56,
804 2394-2403, 2009.
- 805 Levin, L. A., Huggett, C. L., and Wishner, K. F.: Control of deep-sea benthic community structure by
806 oxygen and organic-matter gradients in the eastern Pacific Ocean, *Journal of Marine Research*, 49, 763-
807 800, 1991.
- 808 Lutjeharms, J., and Stockton, P.: Kinematics of the upwelling front off southern Africa, *South African*
809 *Journal of Marine Science*, 5, 35-49, 1987.
- 810 Mariotti, A., Gadel, F., and Giresse, P.: Carbon isotope composition and geochemistry of particulate
811 organic matter in the Congo River (Central Africa): application to the study of Quaternary sediments off
812 the mouth of the river, *Chemical Geology: Isotope Geoscience Section*, 86, 345-357, 1991.
- 813 Meisel, S., Struck, U., and Emeis, K. C.: Nutrient dynamics and oceanographic features in the central
814 Namibian upwelling region as reflected in $\delta^{15}\text{N}$ -signals of suspended matter and surface sediments,
815 *Fossil Record*, 14, 153-169, 2011.
- 816 Mienis, F., De Stigter, H., White, M., Duineveld, G., De Haas, H., and Van Weering, T.: Hydrodynamic
817 controls on cold-water coral growth and carbonate-mound development at the SW and SE Rockall
818 Trough Margin, NE Atlantic Ocean, *Deep Sea Research Part I: Oceanographic Research Papers*, 54, 1655-
819 1674, 2007.
- 820 Mienis, F., De Stigter, H., De Haas, H., and Van Weering, T.: Near-bed particle deposition and
821 resuspension in a cold-water coral mound area at the Southwest Rockall Trough margin, NE Atlantic,
822 *Deep Sea Research Part I: Oceanographic Research Papers*, 56, 1026-1038, 2009.
- 823 Mienis, F., Duineveld, G., Davies, A., Ross, S., Seim, H., Bane, J., and Van Weering, T.: The influence of
824 near-bed hydrodynamic conditions on cold-water corals in the Viosca Knoll area, Gulf of Mexico, *Deep*
825 *Sea Research Part I: Oceanographic Research Papers*, 60, 32-45, 2012.
- 826 Mienis, F., Duineveld, G., Davies, A., Lavaleye, M., Ross, S., Seim, H., Bane, J., Van Haren, H., Bergman,
827 M., and De Haas, H.: Cold-water coral growth under extreme environmental conditions, the Cape
828 Lookout area, NW Atlantic, *Biogeosciences*, 11, 2543, 2014.
- 829 Miller, R. J., Hocevar, J., Stone, R. P., and Fedorov, D. V.: Structure-forming corals and sponges and their
830 use as fish habitat in Bering Sea submarine canyons, *PLoS One*, 7, e33885, 2012.
- 831 Mills, D. B., Francis, W. R., Vargas, S., Larsen, M., Elemans, C. P., Canfield, D. E., and Wörheide, G.: The
832 last common ancestor of animals lacked the HIF pathway and respired in low-oxygen environments,
833 *eLife*, 7, e31176, 2018.
- 834 Mohrholz, V., Bartholomae, C., Van der Plas, A., and Lass, H.: The seasonal variability of the northern
835 Benguela undercurrent and its relation to the oxygen budget on the shelf, *Continental Shelf Research*,
836 28, 424-441, 2008.
- 837 Mohrholz, V., Eggert, A., Junker, T., Nausch, G., Ohde, T., and Schmidt, M.: Cross shelf hydrographic and
838 hydrochemical conditions and their short term variability at the northern Benguela during a normal
839 upwelling season, *Journal of Marine Systems*, 140, 92-110, 2014.
- 840 Montoya, J. P.: Natural abundance of ^{15}N in marine planktonic ecosystems, *Stable isotopes in Ecology*
841 *and Environmental Science*, 176, 2007.
- 842 Mortensen, P. B., Hovland, T., Fosså, J. H., and Furevik, D. M.: Distribution, abundance and size of
843 *Lophelia pertusa* coral reefs in mid-Norway in relation to seabed characteristics, *Journal of the Marine*
844 *Biological Association of the United Kingdom*, 81, 581-597, 2001.



- 845 Mosch, T., Sommer, S., Dengler, M., Noffke, A., Bohlen, L., Pfannkuche, O., Liebetrau, V., and Wallmann,
846 K.: Factors influencing the distribution of epibenthic megafauna across the Peruvian oxygen minimum
847 zone, *Deep Sea Research Part I: Oceanographic Research Papers*, 68, 123-135, 2012.
- 848 Mueller, C., Larsson, A., Veuger, B., Middelburg, J., and Van Oevelen, D.: Opportunistic feeding on
849 various organic food sources by the cold-water coral *Lophelia pertusa*, *Biogeosciences*, 11, 123-133,
850 2014.
- 851 Mullins, H. T., Thompson, J. B., McDougall, K., and Vercoutere, T. L.: Oxygen-minimum zone edge effects:
852 evidence from the central California coastal upwelling system, *Geology*, 13, 491-494, 1985.
- 853 Odum, H. T.: *Environment, power and society*, New York, USA, Wiley-Interscience, 1971.
- 854 Oevelen, D. v., Duineveld, G., Lavaleye, M., Mienis, F., Soetaert, K., and Heip, C. H.: The cold-water coral
855 community as hotspot of carbon cycling on continental margins: A food-web analysis from Rockall Bank
856 (northeast Atlantic), *Limnology and Oceanography*, 54, 1829-1844, 2009.
- 857 Perdue, E. M., and Koprivnjak, J.-F.: Using the C/N ratio to estimate terrigenous inputs of organic matter
858 to aquatic environments, *Estuarine, Coastal and Shelf Science*, 73, 65-72, 2007.
- 859 Pichevin, L., Bertrand, P., Boussafir, M., and Disnar, J.-R.: Organic matter accumulation and preservation
860 controls in a deep sea modern environment: an example from Namibian slope sediments, *Organic*
861 *Geochemistry*, 35, 543-559, 2004.
- 862 Poole, R., and Tomczak, M.: Optimum multiparameter analysis of the water mass structure in the
863 Atlantic Ocean thermocline, *Deep Sea Research Part I: Oceanographic Research Papers*, 46, 1895-1921,
864 1999.
- 865 Rae, C. D.: A demonstration of the hydrographic partition of the Benguela upwelling ecosystem at 26°
866 40'S, *African Journal of Marine Science*, 27, 617-628, 2005.
- 867 Ramos, A., Sanz, J. L., Ramil, F., Agudo, L. M., and Presas-Navarro, C.: The Giant Cold-Water Coral
868 Mounds Barrier Off Mauritania, in: *Deep-Sea Ecosystems Off Mauritania*, edited by: Ramos, A., Ramil, F,
869 Sanz, J.L (Eds.), Springer, 481-525, 2017.
- 870 Roberts, J. M., Wheeler, A. J., and Freiwald, A.: Reefs of the deep: the biology and geology of cold-water
871 coral ecosystems, *Science*, 312, 543-547, 2006.
- 872 Ruhl, H. A.: Community change in the variable resource habitat of the abyssal northeast Pacific, *Ecology*,
873 89, 991-1000, 2008.
- 874 Sanders, H.: Benthic marine diversity and the stability-time hypothesis, *Brookhaven Symposia in Biology*,
875 1969, 71-81,
- 876 Schlitzer, R.: *Ocean Data View*. <http://odv.awi.de>, 2011.
- 877 Schroeder, W.: Observations of *Lophelia pertusa* and the surficial geology at a deep-water site in the
878 northeastern Gulf of Mexico, *Hydrobiologia*, 471, 29-33, 2002.
- 879 Shannon, L., Boyd, A., Brundrit, G., and Taunton-Clark, J.: On the existence of an El Niño-type
880 phenomenon in the Benguela system, *Journal of Marine Research*, 44, 495-520, 1986.
- 881 Shannon, L., Agenbag, J., and Buys, M.: Large-and mesoscale features of the Angola-Benguela front,
882 *South African Journal of Marine Science*, 5, 11-34, 1987.
- 883 Shannon, L., and Nelson, G.: The Benguela: large scale features and processes and system variability, in:
884 *The South Atlantic*, Springer, Berlin, Heidelberg, 163-210, 1996.
- 885 Shannon, L.: Benguela Current, *Ocean Currents: A Derivative of Encyclopedia of Ocean Sciences*, 23-34,
886 2001.
- 887 Sokolova, I. M., Frederich, M., Bagwe, R., Lannig, G., and Sukhotin, A. A.: Energy homeostasis as an
888 integrative tool for assessing limits of environmental stress tolerance in aquatic invertebrates, *Marine*
889 *Environmental Research*, 79, 1-15, 2012.
- 890 Tahey, T., Duineveld, G., Berghuis, E., and Helder, W.: Relation between sediment-water fluxes of
891 oxygen and silicate and faunal abundance at continental shelf, slope and deep-water stations in the
892 northwest Mediterranean, *Marine Ecology Progress Series*, 119-130, 1994.



- 893 Tamborrino, L., Wienberg, C., Titschack, J., Wintersteller, P., Mienis, F., Freiwald, A., Orejas, C., Dullo,
894 W.-C., Haberkern, J., and Hebbeln, D.: Mid-Holocene extinction of cold-water corals on the Namibian
895 shelf steered by the Benguela Upwelling System Submitted to Geology, submitted.
- 896 Taviani, M., Remia, A., Corselli, C., Freiwald, A., Malinverno, E., Mastrototaro, F., Savini, A., and Tursi, A.:
897 First geo-marine survey of living cold-water *Lophelia* reefs in the Ionian Sea (Mediterranean basin),
898 *Facies*, 50, 409-417, 2005.
- 899 Team, R. C.: R: A language and environment for statistical computing [Internet]. Vienna, Austria; 2014.
900 2017.
- 901 Thiem, Ø., Ravagnan, E., Fosså, J. H., and Berntsen, J.: Food supply mechanisms for cold-water corals
902 along a continental shelf edge, *Journal of Marine Systems*, 60, 207-219, 2006.
- 903 Titschack, J., Baum, D., De Pol-Holz, R., Lopez Correa, M., Forster, N., Flögel, S., Hebbeln, D., and
904 Freiwald, A.: Aggradation and carbonate accumulation of Holocene Norwegian cold-water coral reefs,
905 *Sedimentology*, 62, 1873-1898, 2015.
- 906 Tyrrell, T., and Lucas, M. I.: Geochemical evidence of denitrification in the Benguela upwelling system,
907 *Continental Shelf Research*, 22, 2497-2511, 2002.
- 908 van Haren, H., Mienis, F., Duineveld, G. C., and Lavaley, M. S.: High-resolution temperature
909 observations of a trapped nonlinear diurnal tide influencing cold-water corals on the Logachev mounds,
910 *Progress in Oceanography*, 125, 16-25, 2014.
- 911 van Soest, R. W., Cleary, D. F., de Kluijver, M. J., Lavaley, M. S., Maier, C., and van Duyl, F. C.: Sponge
912 diversity and community composition in Irish bathyal coral reefs, *Contributions to Zoology*, 76, 2007.
- 913 Welschmeyer, N. A., and Lorenzen, C. J.: Chlorophyll budgets: Zooplankton grazing and phytoplankton
914 growth in a temperate fjord and the Central Pacific Gyres¹, *Limnology and Oceanography*, 30, 1-21,
915 1985.
- 916 Wheeler, A. J., Beyer, A., Freiwald, A., De Haas, H., Huvenne, V., Kozachenko, M., Olu-Le Roy, K., and
917 Opderbecke, J.: Morphology and environment of cold-water coral carbonate mounds on the NW
918 European margin, *International Journal of Earth Sciences*, 96, 37-56, 2007.
- 919 White, M., Mohn, C., de Stigter, H., and Mottram, G.: Deep-water coral development as a function of
920 hydrodynamics and surface productivity around the submarine banks of the Rockall Trough, NE Atlantic,
921 in: *Cold-water corals and ecosystems*, edited by: A Freiwald, J. R., Springer, Heidelberg, 503-514, 2005.
- 922 White, M., Wolff, G. A., Lundälv, T., Guihen, D., Kiriakoulakis, K., Lavaley, M., and Duineveld, G.: A
923 Freiwald, JM Roberts, Cold-water coral ecosystem (Tisler Reef, Norwegian Shelf) may be a hotspot for
924 carbon cycling, *Marine Ecology Progress Series*, 465, 11-23, 2012.
- 925 Wienberg, C., and Titschack, J.: Framework-forming scleractinian cold-water corals through space and
926 time: a late Quaternary North Atlantic perspective, Ros-si S, Bramanti L, Gori A, Orejas C, *Marine Animal*
927 *Forests: the Ecology of Benthic Biodiversity Hotspots*, Springer, 699-732 pp., 2017.
- 928 Wienberg, C., Titschack, J., Freiwald, A., Frank, N., Lundälv, T., Taviani, M., Beuck, L., Schröder-Ritzrau,
929 A., Krengel, T., and Hebbeln, D.: The giant Mauritanian cold-water coral mound province: Oxygen control
930 on coral mound formation, *Quaternary Science Reviews*, 185, 135-152, 2018.
- 931 Wilson, J.: 'Patch' development of the deep-water coral *Lophelia pertusa* (L.) on Rockall Bank, *Journal of*
932 *the Marine Biological Association of the United Kingdom*, 59, 165-177, 1979.
- 933 Zabel, M., Boetius, A., Emeis, K.-C., Ferdelman, T. G., and Spieß, V.: PROSA Process Studies in the Eastern
934 South Atlantic – Cruise No. M76 – April 12 – August 24, 2008 – Cape Town (South Africa) – Walvis Bay
935 (Namibia). , DFG Senatskommission für Ozeanographie, METEOR-Berichte, M76, 180 pp., 2012.

936 11. Figure captions

937 **Figure 1** (a) Overview map showing the research areas off Angola and Namibia (red squares) and main features of the surface
938 water circulation (arrows) and frontal zone (dashed line) in the SE Atlantic as well as the two main rivers discharging at the



939 Angolan margin. Detailed bathymetry maps of the Angolan (upper maps) and Namibian margins (lower maps) showing the
940 position of (b) CTD transects (note the deep CTD cast down to 1000 m water depth conducted off Namibia) and (c) bottom
941 lander deployments (red squares shown in b indicate the cutouts displayed in c).

942 **Figure 2** ROV images (copyright MARUM ROV SQUID, Bremen, Germany) showing the surface coverage of cold-water coral
943 mounds discovered off Namibia (a, b) and Angola (c, d). Images were recorded and briefly described for their faunal
944 composition during RV *Meteor* cruise M122 "ANNA" (see Hebbeln et al. 2017). (a) Sylvester mound, 225 m water depth. Dead
945 coral framework entirely consisting of *Lophelia pertusa*. The framework is intensely colonized by the yellow bryozoan
946 *Metropririella* sp., zoanithids, actiniarians and sponges. Vagile fauna consists of asteroids and gobiid fishes (*Sufflogobius*
947 *bibarbatus*) that hide between hollows underneath the coral framework. (b) Sylvester mound, 238 m water depth. Dense coral
948 rubble (*L. pertusa*) heavily overgrown by *Metropririella* sp. and sponges. Note the decapod crab *Macropipus australis* (center of
949 the image). (c) Valentine mound, 238 m water depth. Live *Lophelia* colony being grazed by echinoids. Note the sponge
950 *Aphrocallistes* sp. with its actinarian symbionts (right side of the image). (d) Buffalo mound, 345 m water depth. Living CWC
951 reef observed on top of an Angolan coral mound. Many fishes are present around the reef (*Helicolenus dactylopterus*,
952 *Gephyroberyx darwinii*).

953 **Figure 3** TS-diagrams showing the different water masses being present at the (a) Namibian and (b) Angolan margins: South
954 Atlantic Subtropical Surface Water (SASSW), South Atlantic Central Water (SACW) and Eastern South Atlantic Central water
955 (ESACW), Antarctic Intermediate Water (AAIW) (data plotted using Ocean Data View v.4.7.8; <http://odv.awi.de>; Schlitzer, 2011).
956 Red dotted line indicates the depth range of cold-water coral mound occurrence.

957 **Figure 4** CTD transect across the Namibian margin. Shown are data for: (a) potential temperature ($^{\circ}\text{C}$), (b) salinity (PSU), (c)
958 dissolved oxygen concentrations (ml l^{-1}), note the pronounced oxygen minimum zone (OMZ) between 100-335 m water depth,
959 and d) fluorescence (mg m^{-3}) (data plotted using Ocean Data View v.4.7.8; <http://odv.awi.de>; Schlitzer, 2011). The occurrence of
960 fossil CWC mounds is indicated by a red dashed line, colored dots indicate bottom lander deployments.

961 **Figure 5** Data recorded by the ALBEX lander (210 m) at the Namibian margin in January 2016. Shown are data for temperature
962 ($^{\circ}\text{C}$; red), dissolved oxygen concentrations (ml l^{-1} ; blue), optical backscatter (turbidity; moss green), fluorescence (counts per
963 second green), current speed (m s^{-1} ; pink), current direction (degree: 0-360 $^{\circ}$; dark red) as well as nitrogen (mg l^{-1} ; pink dots),
964 carbon (mg l^{-1} ; purple dots), and chlorophyll- α concentration ($\mu\text{g l}^{-1}$; green dots) of SPOM collected during the first 48h by the
965 McLane pump. These data are supplemented by wind speed and direction (small black arrows) recorded concurrently to the
966 lander deployment by ship bound devices. Note that current directions changed from a generally south-poleward to an
967 equatorward direction when wind speed exceeded 10 m s^{-1} (stormy period indicated by black arrow).

968 **Figure 6** Composite records of SPOM collected by the McLane pump of the ALBEX lander at the Namibian and Angolan margins
969 during all three deployments. (a) $\delta^{15}\text{N}$ and $\delta^{13}\text{C}$ isotopic values at the Namibian (red dots) and Angolan (blue and green dots)
970 margins. Indicated by the square boxes are common isotopic values of terrestrial and marine organic matter (Boutton 1991,
971 Holmes et al. 1997, Sigman et al. 2009). The relative contribution of terrestrial material (green boxes) is increasing with a more
972 negative $\delta^{13}\text{C}$ value. (b) Total organic carbon (TOC) and nitrogen (N) concentration of the SPOM. Values of the Namibian
973 margin are marked by a blue circle (C/N ratio = 7.8), values of the Angolan margin are marked by a green circle (C/N ratio = 9.6).
974 Dissolved oxygen concentrations are included to show the higher nutrient concentrations in less oxygenated water.



975 **Figure 7** CTD transect across the Angolan margin. Shown are data for (a) potential temperature ($^{\circ}\text{C}$), (b) salinity (PSU), (c)
 976 dissolved oxygen concentration (ml l^{-1}), (d) fluorescence (mg m^{-3}), (e) turbidity (NTU) (data plotted using Ocean Data View
 977 v.4.7.8; <http://odv.awi.de>; Schlitzer, 2011). The depth occurrence of CWC mounds is marked by a red, dashed line, the lander
 978 deployments are indicated by colored dots.

979 **Figure 8** Lander data (ALBEX) recorded during the shallow (~ 340 m water depth) and deep deployments (~ 530 m water depth)
 980 off Angola (January 2016). Shown are temperature ($^{\circ}\text{C}$; red), dissolved oxygen concentration (ml l^{-1} ; blue), fluorescence (counts
 981 per second; green), optical backscatter (turbidity; yellow), current speed (m s^{-1} ; pink) and current direction (degree: $0\text{--}360^{\circ}$;
 982 purple) as well as nitrogen (mg l^{-1} ; pink dots), carbon (mg l^{-1} ; purple dots), and chlorophyll- α concentration ($\mu\text{g l}^{-1}$; green dots) of
 983 SPOM collected during the both deployments by the McLane pump.

984 **Figure 9** Depth range of cold-water coral mound occurrences (blue shaded areas) at the (a) Namibian and (b) Angolan margins
 985 in relation to the dissolved oxygen concentrations and potential temperature. Diurnal tides are delivering mainly phytodetritus
 986 (shown in (a) and organic matter from the benthic nepheloid layer (shown in (b) as well as oxygen from above, and from below
 987 to the mound sites (indicated by blue arrows, the length of which indicate the tidal ranges).

988 12. Tables

989 **Table 1.** Metadata of lander deployments conducted during RV *Meteor* cruise M122 (ANNA) in January 2016. The deployment
 990 sites are shown in Figure 1.

	Station no. (GeoB ID)	Area	Lander	Date	Latitude [S]	Longitude [E]	Depth [m]	Duration [days]	Devices
Namibia	20507-1	on-mound	ALBEX	01.- 09.01.16	$20^{\circ}44.03'$	$12^{\circ}49.23'$	210	7.8	+ particle pump
	20508-1	off-mound	TROL	01.- 09.01.16	$20^{\circ}44.03'$	$12^{\circ}49.14'$	220	7.8	
	20506-1	off-mound	SLM	01.- 16.01.16	$20^{\circ}43.93'$	$12^{\circ}49.11'$	231	12.5	
Angola	20921-1	off-mound	ALBEX	20.- 23.01.16	$9^{\circ}46.16'$	$12^{\circ}45.96'$	342	2.5	+ particle pump
	20940-1	off-mound	ALBEX	23.- 26.01.16	$9^{\circ}43.84'$	$12^{\circ}42.15'$	532	2.6	+ particle pump
	20916-1	off-mound	TROL	19.- 26.01.16	$9^{\circ}43.66'$	$12^{\circ}42.09'$	526	6.8	
	20915-2	off-mound	SLM	19.- 26.01.16	$9^{\circ}43.87'$	$12^{\circ}43.87'$	430	6.8	

991

992 **Table 2** Tidal analysis of the ALBEX lander from 6 m above the sea floor. Depth, mean current speed, polarization ratio, mean
 993 current direction, tidal prediction of pressure fluctuations, two most important harmonics with amplitude, tidal prediction of
 994 horizontal current field, two most important harmonics with semi-major axis' amplitude.



	Station no. (GeoB ID)	Depth (m)	Mean current speed (cm s ⁻¹)	Polarization ratio	Current direction (°)	Tides [%] (p)	Const. [dbar]	Tides [%] (u)	Const. [cm s ⁻¹]
Namibia	20507-1	433	9.34	0.18	221.6	81.8	M2: 0.37	10.5	M2: 3.1 M3: 0.8
Angola	20921-1	532	9.96	0.42	247.9	91.6	M2: 0.59 M3: 0.04	36	M2: 7.8 M8: 0.7
	20940-1	228	8.92	0.86	275.6	86.8	M2: 0.60 M8: 0.02	50.9	M2: 8.6 M3: 3.7

995

996